Article

Cell Metabolism

Combined Inhibition of DYRK1A, SMAD, and Trithorax Pathways Synergizes to Induce Robust Replication in Adult Human Beta Cells

Graphical Abstract

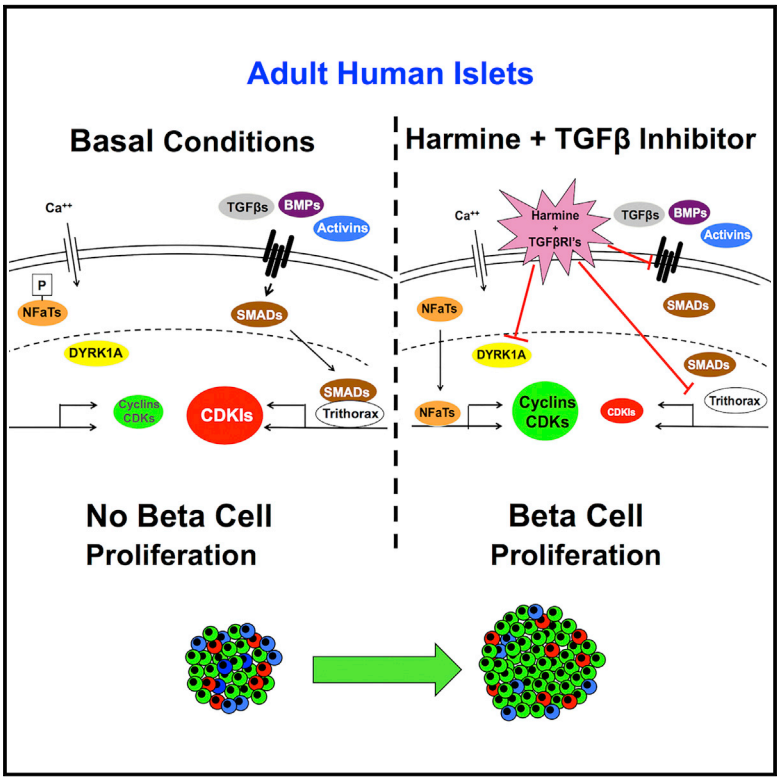

Authors

Peng Wang, Esra Karakose, Hongtao Liu, ..., Donald K. Scott, Adolfo Garcia-Ocaña, Andrew F. Stewart

Correspondence

andrew.stewart@mssm.edu

In Brief

Adult human pancreatic beta cells are notoriously resistant to replication. Wang et al. find that the combination of the DYRK1A inhibitor harmine with an inhibitor of the TGFβ superfamily of receptors induces synergistic increases in human beta cell cells *in vitro* and *in vivo* associated with enhanced differentiation.

Highlights

- Adult human pancreatic beta cells can be induced to proliferate at high rates
- Driven by synergy between DYRK1A inhibitors and TGFβ superfamily inhibitors
- Reflects activation of cyclins and CDKs accompanied by CDK inhibitor suppression
- Proliferation occurs in type 2 diabetic beta cells, with enhanced differentiation

Wang et al., 2019, Cell Metabolism *29*, 1–15
March 5, 2019
https://doi.org/10.1016/j.cmet.2018.12.005

CellPress

Please cite this article in press as: Wang et al., Combined Inhibition of DYRK1A, SMAD, and Trithorax Pathways Synergizes to Induce Robust Replication in Adult Human Beta Cells, Cell Metabolism (2018), https://doi.org/10.1016/j.cmet.2018.12.005

Cell Metabolism
Article

Combined Inhibition of DYRK1A, SMAD, and Trithorax Pathways Synergizes to Induce Robust Replication in Adult Human Beta Cells

Peng Wang,[1,5] Esra Karakose,[1,5] Hongtao Liu,[1] Ethan Swartz,[1] Courtney Ackeifi,[1] Viktor Zlatanic,[1] Jessica Wilson,[1] Bryan J. González,[3] Aaron Bender,[1] Karen K. Takane,[1] Lillian Ye,[4] George Harb,[4] Felicia Pagliuca,[4] Dirk Homann,[1] Dieter Egli,[3] Carmen Argmann,[2] Donald K. Scott,[1] Adolfo Garcia-Ocaña,[1] and Andrew F. Stewart[1,6,*]

[1]Diabetes, Obesity, and Metabolism Institute, Icahn School of Medicine at Mount Sinai, New York, NY 10029, USA
[2]Department of Genetics and Genomic Sciences, Icahn Institute for Genomics and Multiscale Biology, Icahn School of Medicine at Mount Sinai, New York, NY 10029, USA
[3]Naomi Berrie Diabetes Center, Columbia University, New York, NY 10032, USA
[4]Semma Therapeutics, Cambridge, MA 02142, USA
[5]These authors contributed equally
[6]Lead Contact
*Correspondence: andrew.stewart@mssm.edu
https://doi.org/10.1016/j.cmet.2018.12.005

SUMMARY

Small-molecule inhibitors of dual-specificity tyrosine-regulated kinase 1A (DYRK1A) induce human beta cells to proliferate, generating a labeling index of 1.5%–3%. Here, we demonstrate that combined pharmacologic inhibition of DYRK1A and transforming growth factor beta superfamily (TGFβSF)/SMAD signaling generates remarkable further synergistic increases in human beta cell proliferation (average labeling index, 5%–8%, and as high as 15%–18%), and increases in both mouse and human beta cell numbers. This synergy reflects activation of cyclins and cdks by DYRK1A inhibition, accompanied by simultaneous reductions in key cell-cycle inhibitors (*CDKN1C* and *CDKN1A*). The latter results from interference with the basal Trithorax- and SMAD-mediated transactivation of *CDKN1C* and *CDKN1A*. Notably, combined DYRK1A and TGFβ inhibition allows preservation of beta cell differentiated function. These beneficial effects extend from normal human beta cells and stem cell-derived human beta cells to those from people with type 2 diabetes, and occur both *in vitro* and *in vivo*.

INTRODUCTION

Inhibition of the enzyme dual-specificity tyrosine phosphorylation-regulated kinase 1A (DYRK1A) in human beta cells, using drugs such as harmine, INDY, GNF4877, 5-iodotubericidin (5-IT), or CC-401, is able to induce proliferation (labeling indices) in the 1.5%–3% range, as assessed using Ki67, EdU, BrdU, and/or PCNA immunolabeling of insulin-containing cells derived from human cadaveric islets (Aamodt et al., 2016; Abdolazimi et al., 2018; Dirice et al., 2016; Shen et al., 2015; Wang et al., 2015a, 2016). This notable accomplishment, confirmed in multiple laboratories, replicates the proliferation "rate" in human beta cells in the first year of life, the only stage of human development at which appreciable beta cell proliferation occurs (Gregg et al., 2012; Kassem et al., 2000; Meier et al., 2008; Wang et al., 2015b). One can reasonably assume that more rapid beta cell proliferation would be attractive in order to replete or restore beta cell mass to normal in people with type 1 and type 2 diabetes. Since complete silencing of DYRK1A in human beta cells does not appreciably further increase proliferation (Dirice et al., 2016; Wang et al., 2015a), we surmised that combination treatment with other classes of potential beta cell mitogenic small molecules might enhance efficacy of harmine analogs. We selected TGFβSF receptor inhibitors for combination therapy for several reasons. First, in genomic and transcriptomic analyses of beta cell mitogenic pathways in human insulinoma, SMAD signaling and chromatin remodeling pathways were the most statistically significant (Wang et al., 2017). Second, as described below, we observed that TGFβSF members were abundant in isolated human beta cells, and some were affected by pharmacologic DYRK1A inhibition. Third, Gittes et al.; Kim et al.; Bhushan, Kulkarni et al.; Schneyer et al.; Teramoto et al.,; and Annes et al. (Abdolazimi et al., 2018; Brown and Schneyer, 2010; Brown et al., 2014; Dhawan et al., 2016; El-Gohary et al., 2014; Mukherjee et al., 2007; Nomura et al., 2014; Smart et al., 2006; Xiao et al., 2014, 2016; Zhou et al., 2013) have each reported that genetic or pharmacologic TGFβSF pathway inhibition in rodent beta cells can lead to rodent beta cell proliferation.

Transforming growth factor beta superfamily (TGFβSF) signaling is complex (Antebi et al., 2017; Brown and Schneyer, 2010; Brown et al., 2014; Dhawan et al., 2016; El-Gohary et al., 2014; Gaarenstroom and Hill, 2014; Macias et al., 2015; Mukherjee et al., 2007; Nomura et al., 2014; Smart et al., 2006; Stewart et al., 2015; Xiao et al., 2014, 2016; Zhou et al., 2013). In its simplest form, it involves a series of ligands (e.g., TGFβs 1,2,3, activins, inhibins, glia-derived factors, and bone morphogenic proteins), a series of cognate receptors, and a repertoire of endogenous inhibitors (e.g., sclerostin and follistatin-like factors) that signal downstream through a series of activating or receptor R-SMADs (SMADs 1,2,3,5,8/9) and the co-SMAD, SMAD4, and

are blocked by one of two inhibitory I-SMADs (SMADs 6,7). Once activated, R-SMAD heteromers translocate to the nucleus, where they serve individually or in complexes to transactivate or repress target genes. Notably, at some of these loci, SMADs integrate into epigenetic chromatin-modifying complexes, such as the trithorax group complex (TrxG) that includes histone methylases (e.g., MEN1) and histone demethlyases (e.g., KDM6A) that regulate chromatin access (Antebi et al., 2017; Brown and Schneyer, 2010; Brown et al., 2014; Dhawan et al., 2016; El-Gohary et al., 2014; Gaarenstroom and Hill, 2014; Macias et al., 2015; Mukherjee et al., 2007; Nomura et al., 2014; Smart et al., 2006; Stewart et al., 2015; Xiao et al., 2014, 2016; Zhou et al., 2013).

In this report, we demonstrate that combined pharmacologic or genetic inhibition of DYRK1A and TGFβSF signaling induces remarkable and previously unattainable rates of human beta cell proliferation *in vitro* and *in vivo*, and actually increases human and mouse beta cell numbers. We explore the underlying mechanisms that drive this remarkable rate of proliferation and show that the results apply not only to beta cells from normal cadaveric human islets, but also to human stem cell (hESC)-derived beta cells, and those from people with type 2 diabetes.

RESULTS

Combinations of DYRK1A Inhibitors and TGFβSF Inhibitors Induce Synergistic Human Beta Cell Proliferation and Increase Beta Cell Numbers

Gene expression profiles from fluorescence-activated cell sorting (FACS)-sorted human beta cells (Wang et al., 2017) were remarkable for the abundance of select members of the TGFβSF. In addition, harmine treatment of human islets resulted in notable changes in TGFβSF members (Tables S1 and S2). Reasoning from these observations, from the prominence of SMAD signaling in human insulinoma cell proliferation (Wang et al., 2017), and from the beneficial effects of TGFβ signaling inhibition in mouse islets described by Bhushan, Gittes, Kim, Schneyer, and Teramoto et al. (Brown and Schneyer, 2010; Brown et al., 2014; Dhawan et al., 2016; El-Gohary et al., 2014; Mukherjee et al., 2007; Nomura et al., 2014; Smart et al., 2006; Xiao et al., 2014, 2016; Zhou et al., 2013), we explored the effects of TGFβSF pharmacologic inhibitors on human beta cell proliferation in a large number of human cadaveric islet preparations (Figures 1A–1C). Vehicle alone (DMSO) had no effect, and harmine displayed its usual ~2% labeling index (Wang et al., 2015a), as assessed using Ki67 labeling of insulin-positive cells. A broad range of TGFβ receptor, BMP receptor, and activin receptor inhibitors had little effect on human beta cell proliferation, as previously reported (Dhawan et al., 2016). In contrast, every TGFβSF receptor inhibitor tested, whether targeting TGFβ, activin, or BMP receptors, when used in combination with harmine, induced dramatic increases in the Ki67 labeling index in human beta cells. Proliferation rates (labeling indices) averaged in the 5%–8% range; the large error bars reflect even higher proliferation rates in occasional human islet preparations, sometimes achieving Ki67 labeling indices as high as 15%–18%. These results were independently confirmed using automated, high-throughput, high-content imaging of human HUES8 hESC-derived beta cells (Figure S1) (Pagliuca et al., 2014).

The beneficial effects were not confined to harmine, but extended to additional DYRK1A inhibitors, including INDY and leucettine-41 (Tahtouh et al., 2012) (Figures 1D and 1E). In addition, in dose-response studies, the combinations fulfilled formal criteria for pharmacologic synergy (Figures S2A and S2B). Further, the remarkable synergy could be observed with two additional measures of proliferation: BrdU incorporation and phospho-histone-H3 immunolabeling (Figures 1F, 1G, S2C, and S2D).

Notably, the mitogenic effects of the combination were not specific to beta cells: frequent proliferation was observed in alpha, delta, PP, ductal, and other non-beta cells within the islet as well (Figure 1B, red arrows; Figures S3A and S3B). No adverse effects were observed with respect to beta cell death or DNA damage, as assessed by TUNEL assay and γH2AX immunolabeling, respectively (Figures S3C–S3E).

We next examined whether harmine together with the TGFβ inhibitor LY364947 could increase actual numbers of human beta cells, using two different approaches. First, using adult human cadaveric islets, we employed flow cytometry to count the numbers of live human beta cells, previously labeled with an insulin promoter-driven adenovirus expressing the bright green fluorescent protein ZsGreen (Wang et al., 2017), following 4 days of exposure to vehicle or the harmine-LY364947 combination. As illustrated in Figure 1H, absolute beta cell numbers increased in six of seven human islet preparations treated with the harmine-LY364947 combination, as compared to the same human islets treated with vehicle. Second, to confirm these results independently, we used Mel1 hESCs expressing GFP in one allele of the insulin locus (Micallef et al., 2012), differentiated into beta cells (Sui et al., 2018). Figure 1I illustrates the dramatic increase in absolute GFP^+ cell numbers in these hESC-derived cultures. Together, these findings demonstrate that the harmine-LY364947 combination can increase not only markers of beta cell proliferation, but actual numbers of both stem cell-derived and adult human beta cells.

Harmine-TGFβSF Inhibitor Combinations Enhance Markers of Human Beta Cell Differentiation in Normal and Type 2 Diabetes Islets

Concerned that activation of mitogenic pathways might lead to de-differentiation of beta cells, we explored gene expression of a panel of markers of beta cell differentiation (Figures 2A and 2B). As we had observed for harmine alone (Wang et al., 2015a), not only did the harmine-TGFβSF inhibitor combination fail to induce de-differentiation, but the opposite occurred: gene expression of key beta cell markers such as *PDX1*, *NKX6.1*, *MAFA*, *MAFB*, *SLC2A2*, and *PCSK1* all increased with combined harmine-TGFβSF inhibitor treatment, as assessed on whole islets by qPCR; *ISL1*, *SLC2A1*, *NEUROD*, *NKX2.2*, and *PCSK2* all remained the same as at baseline. Only *PAX4* declined, the significance of which is uncertain. These results were confirmed and expanded using massively parallel RNA sequencing (RNA-seq) of human cadaveric islets treated with the harmine-TGFβSF inhibitor combination (Tables S1 and S2). Immunocytochemistry in dispersed human islet preparations confirmed the increases in PDX1, NKX6.1, and MAFA specifically in human beta cells

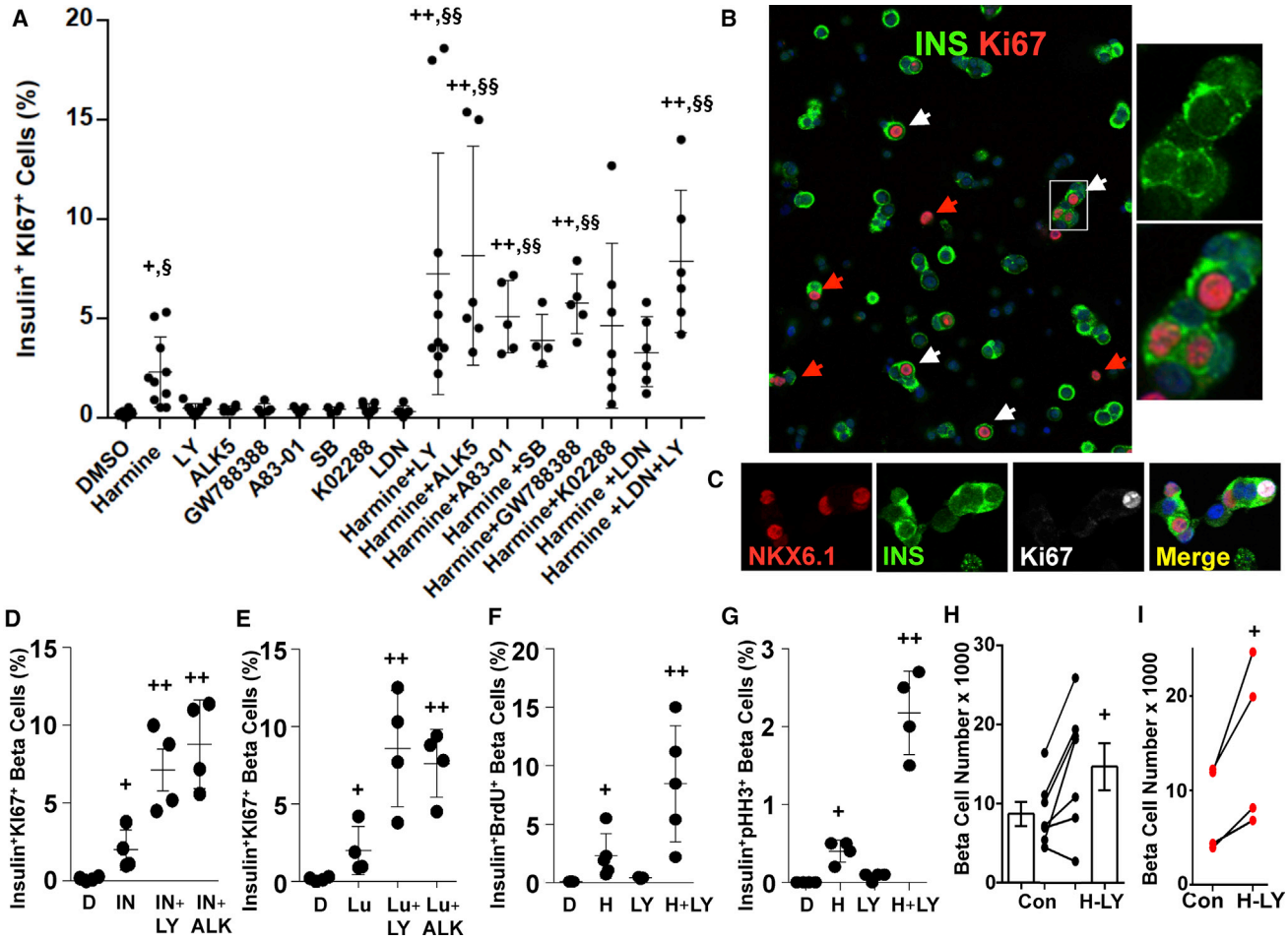

Figure 1. Induction of Human Beta Cell Proliferation and Augmentation of Beta Cell Numbers by Combined Harmine and TGFβSF Inhibitor Treatment

(A) The effects of harmine alone, and of various TGFβSF ligand inhibitors, some of which are specific for TGFβ receptors, and others for activin, inhibin, and BMP receptors. As can be seen, and as reported previously (Aamodt et al., 2016; Abdolazimi et al., 2018; Dirice et al., 2016; Shen et al., 2015; Wang et al., 2015a, 2016), harmine induces Ki67 labeling in approximately 2% of normal human beta cells, and TGFβSF inhibitors lead to only marginal Ki67 labeling. However, each of the TGFβSF inhibitors in combination with harmine induces striking increases in Ki67 labeling in beta cells.

(B) Examples of human islets, treated with the harmine-LY364947 combination, immunolabeled for insulin− (green) and Ki67− (red), exemplifying unprecedented rates of proliferation. The white arrows illustrate beta cells labeled with Ki67; the red arrows indicate other non-beta cell types that are Ki67+. The panels on the right are enlarged from the white box within the main figure.

(C) Examples of NKX6.1, insulin, and Ki67 and a merged view illustrating co-immunolabeling of Ki67 and NKX6.1 in insulin+ cells.

(D and E) The effects of two other harmine analogs, INDY (IN) (Wang et al., 2015a) (D) and leucettine-41 (Lu) (Tahtouh et al., 2012) (E), on human beta cell labeling with Ki67 with or without addition of TGFβ inhibitors LY and ALK5.

(F and G) The effects of harmine and LY364947 alone or in combination on human islets using BrdU (overnight exposure) (F) and phospho-histone-3 (PHH3) (G). Examples of photomicrographs are provided in Figures S2C and S2D. Note that PHH3 captures only G2M phases of cell cycle, as compared to Ki67 and BrdU, which capture all phases of cell cycle, so that labeling indices for PHH3 are lower than for Ki67 and BrdU.

(H) Effect of the harmine-LY combination on adult human beta cell numbers as assessed by FACS counting using an internal recovery standard, Spherotech beads.

(I) Effects of the harmine-LY combination on numbers of Mel1-hESC-derived beta cells from four different batches of cells. Each pair of dots connected by a line represents one batch of hESC-derived beta cells.

In all panels, drug treatments were for 96 hr, and all experiments were done on dispersed islets. In (A) and (D)–(I), each black dot represents an individual human islet preparation. Numbers of donors and beta cells counted are provided in Table S3. For all panels, $^{+}p < 0.05$ versus control by paired t test, and $^{\S}p < 0.05$ by ANOVA. $^{++}p < 0.05$ versus harmine treatment by paired t test, and $^{\S\S}p < 0.05$ versus harmine by ANOVA.

(Figures 2C and S4A). Further, RNA-seq demonstrated that so-called disallowed or forbidden beta cell genes (Pullen and Rutter, 2013; Schuit et al., 2012) were not altered by the harmine-TGFβSF inhibitor combination (Table S2). In line with the observations above, glucose-stimulated insulin secretion was normal, and possibly accentuated, in human islets treated with the harmine-TGFβSF inhibitor combination (Figure 2D).

Since de-differentiation of beta cells occurs in both mice and humans with type 2 diabetes (Cinti et al., 2016; Talchai et al.,

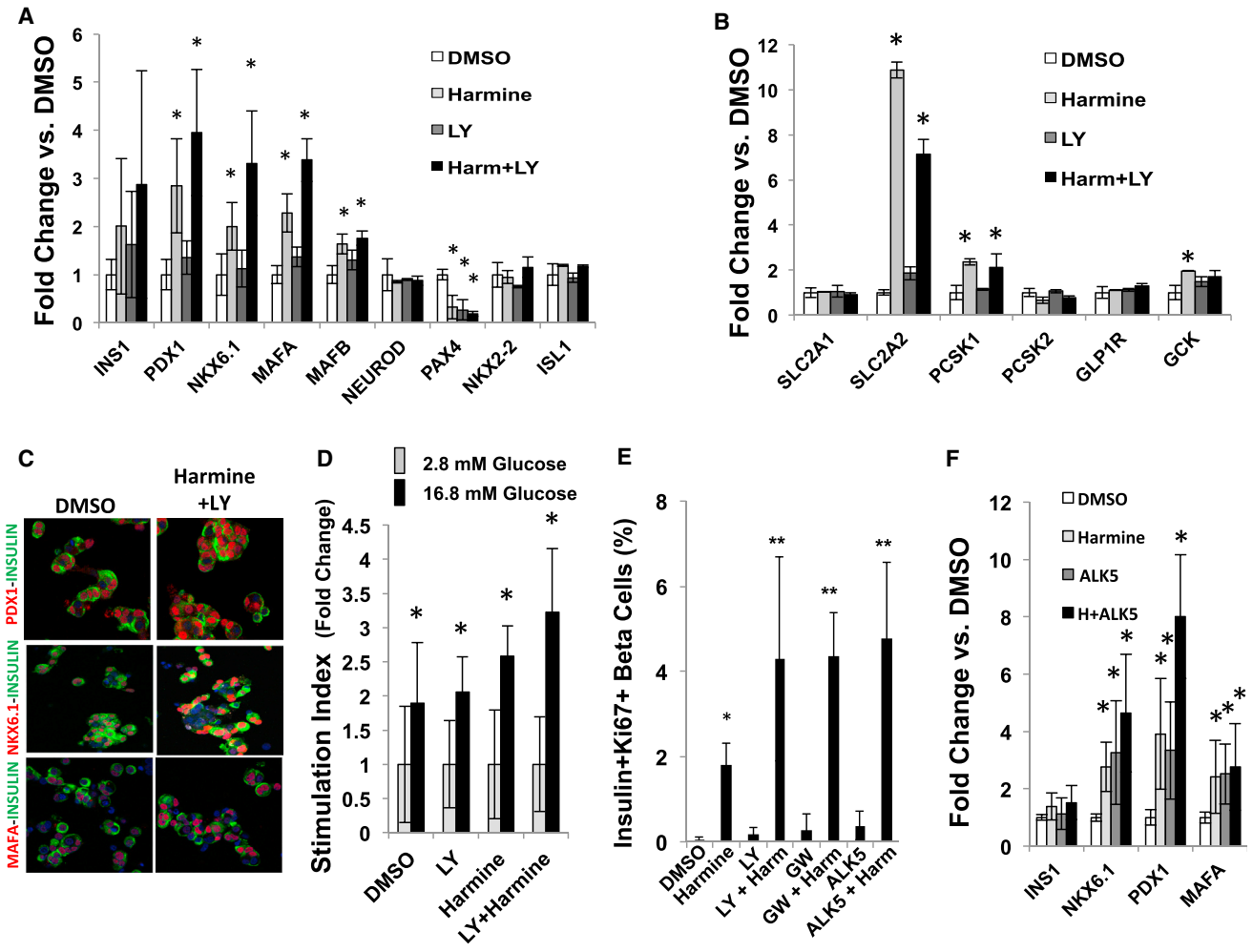

Figure 2. The Harmine-TGFβSF Inhibition Combination Increases Beta Cell Differentiation Markers in Normal and Type 2 Diabetes Beta Cells

(A and B) Effects of harmine and the harmine-LY364947 combination treatment for 4 days on key beta cell transcription factors (A) and markers of beta cell differentiation (B) in whole human islets assessed by qPCR. The panels include five human islet preparations. *$p < 0.05$ versus vehicle (DMSO) treatment.

(C) Immunocytochemistry on dispersed human beta cells (green) showing that combination treatment increases PDX1, NKX6.1, and MAFA (red) specifically in beta cells. Representative of experiments in three different human islet donor preparations. Brighter images are shown in Figure S4A.

(D) Insulin secretion in response to low and high glucose in islets from eight different donors in the presence of vehicle, harmine, LY364947, or the harmine-LY364947 combination. *$p < 0.05$ for high glucose versus low glucose.

(E) Effects of harmine and TGFβ inhibitors on beta cell Ki67 immunolabeling in islets from six donors with type 2 diabetes. *$p < 0.05$ versus control. **$p < 0.05$ versus harmine.

(F) Effects of harmine alone and with ALK5 on key beta cell transcription factors and markers in whole islets from six donors with type 2 diabetes, as assessed by qPCR. Effects of additional TGFβ inhibitors on type 2 diabetes islets are shown in Figure S4B. *$p < 0.05$ versus control.

All drug treatments were for 96 hr, and all experiments were performed on dispersed islets, except for (D), which employed whole islets. Error bars in all panels indicate mean ± SEM. Numbers of donors and beta cells counted are provided in Table S3.

2012), we next explored proliferation in islets derived from six donors with type 2 diabetes (Figure 2E). Remarkably, harmine alone increased Ki67 immunolabeling to the same degree observed in non-diabetic islet donors (Wang et al., 2015a). Moreover, harmine in combination with three different TGFβSF inhibitors (LY364947, ALK5, and GW788388) led to synergistic increases in Ki67 labeling, as had been observed in normal islets (Figures 1 and 2). Equally remarkably, harmine in combination with the TGFβSF inhibitor ALK5 also led to significant increases in expression of *PDX1*, *NKX6.1*, and *MAFA* in human type 2 diabetes islets (Figure 2F), results that extend to the combination of harmine plus GW788388 or LY364947 (Figure S4B).

Combined Harmine-TGFβSF Inhibition Efficacy Requires SMAD and DYRK1A Signaling

TGFβSF ligands affect SMAD signaling but may also recruit other signaling pathways (Antebi et al., 2017; Brown and Schneyer, 2010; Stewart et al., 2015). To ascertain whether the harmine-TGFβSF inhibitor combination affected SMAD signaling, human islets were incubated with harmine alone or in combination with two TGFβSF inhibitors, LY364947 or

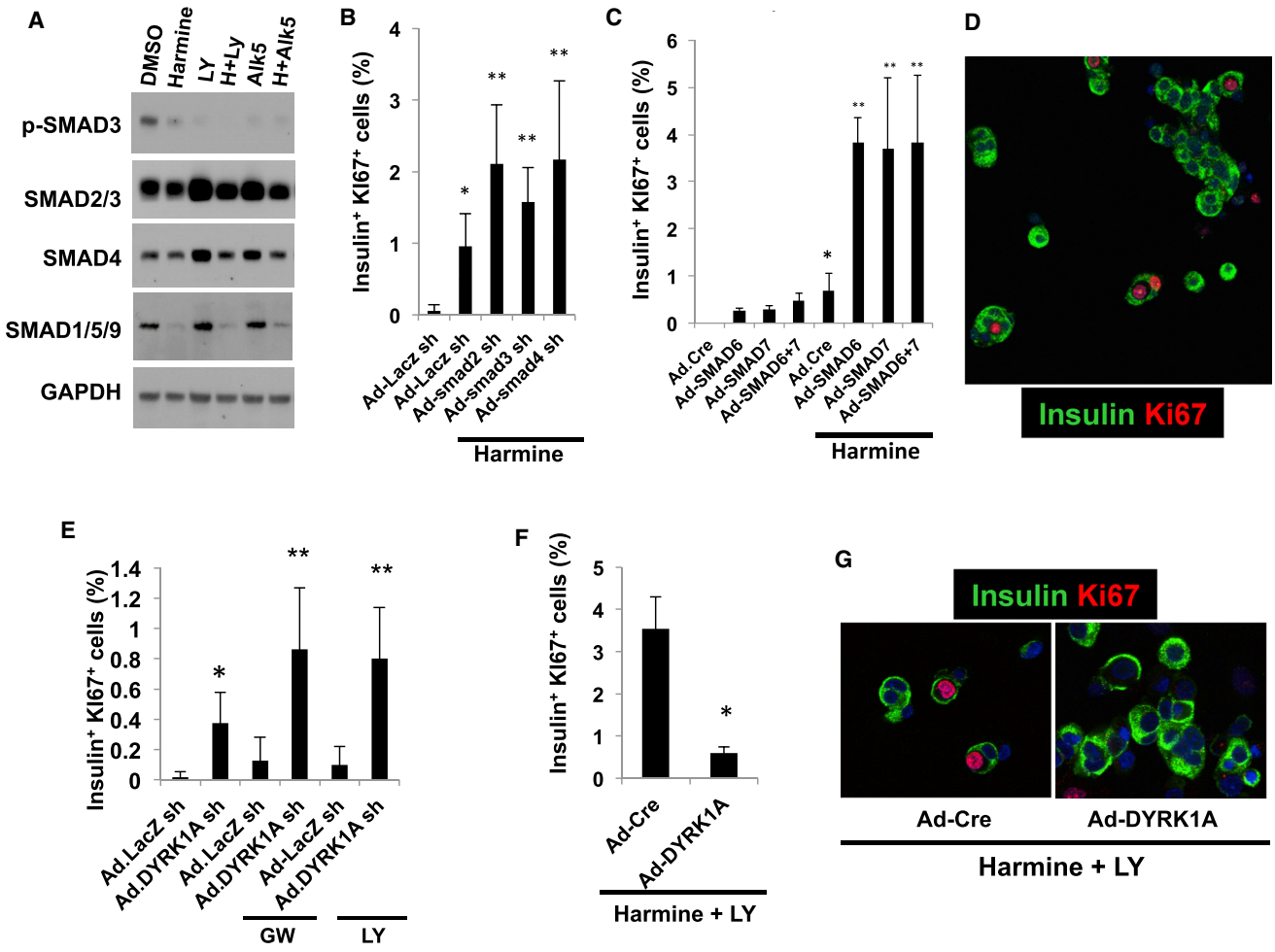

Figure 3. Requirements for DYRK1A and SMAD Signaling

(A) Immunoblots of control, harmine-, LY364947-, ALK5 inhibitor-, or combination-treated whole human islets. While SMAD2 and SMAD3 (detected by the same antibody) did not change, p-SMAD3 was reduced by harmine, and further reduced by LY364947 or ALK5 inhibitor and the combinations. SMAD1, 5, and 9 are also detected by a common antibody, and are reduced by harmine and the drug combinations. The immunoblots are representative of separate experiments in human islets from three different donors.

(B) Effects of a control adenovirus expressing an shRNA directed against LacZ and adenoviruses silencing SMAD2, 3, and 4 (150 MOI each) on Ki67 immunolabeling in harmine-treated human islets.

(C) Effects of adenoviral SMAD6 and SMAD7 overexpression (100 MOI each) on beta cell proliferation, alone and in combination with harmine.

(D) An example of the mitogenic effects of SMAD7 silencing in human beta cells (green) on Ki67 immunolabeling.

(E) The effects of adenoviral silencing of DYRK1A in combination with TGFβSF inhibitors GW788388 or LY364947. Ad.shLacZ indicates a control sh-adenovirus for the Ad.shDYRK1A.

(F) Effect of adenoviral DYRK1A overexpression or a control adenovirus expressing Cre (Ad.Cre) on proliferation in human islets treated with the harmine-LY364947 combination.

(G) Examples of Ad.Cre- and Ad.DYRK1A-overexpressing viruses on Ki67 immunolabeling in human islets treated with harmine and LY364947. All adenovirus experiments were for 96 hr, and all experiments were done on dispersed islets.

In all panels, error bars represent mean ± SEM, *$p < 0.05$ versus control, and **$p < 0.05$ versus harmine. Numbers of donors and beta cells counted are provided in Table S3.

ALK5, and the expression levels of various SMADs were assessed (Figure 3A). The harmine-TGFβSF inhibitor combinations led to reductions in SMAD3 phosphorylation without altering SMAD2/3 abundance, and also led to dramatic reductions in total SMADs 1/5/9 (note that antisera do not distinguish between these three SMADs). Perhaps most interestingly, harmine alone led to reductions in phospho-SMAD3 as well as to reductions in total SMAD1/5/9, a result that extends the apparent reduced expression of select TGFβSF members noted earlier in Table S2.

To explore the requirement for SMAD signaling in the proliferation induced by the harmine-TGFβSF inhibitor combinations, we used adenoviruses expressing short hairpin RNAs (shRNAs) directed against the R-SMADs 2 and 3 and their co-SMAD, SMAD4, in human islets treated with harmine (Figure 3B). We observed that silencing these three R-SMADs further enhanced

harmine-induced human beta cell proliferation. Conversely, overexpressing the I-SMADs 6 and 7 by themselves had no effect on proliferation, but markedly enhanced harmine-induced proliferation (Figures 3C and 3D). Collectively, these results reveal three key insights. First, the proliferation generated by the TGFβSF inhibitors when given in combination with harmine is mediated in large part or entirely via SMAD signaling, since silencing R-SMADs or overexpressing I-SMADs was able to substitute for TGFβSF inhibitors in the combination. Second, harmine itself has previously unrecognized inhibitory effects on SMAD signaling at the protein level (SMADs1/5/9 and phospho-SMAD3). And third, multiple SMAD families (i.e., both the canonical TGFβ receptor-associated SMADs 2,3,4 and the canonical BMP receptor-associated SMADs 1,5,8/9) participate in harmine-mediated proliferation.

Harmine analogs derive their mitogenic effects in large part, if not exclusively, via inhibition of DYRK1A (Abdolazimi et al., 2018; Dirice et al., 2016; Shen et al., 2015; Wang et al., 2015a). To explore the presumed requirement for DYRK1A in the synergistic proliferation derived from the harmine-TGFβ inhibitor combination, we employed adenoviral silencing and overexpression of DYRK1A, alone or in combination with TGFβSF inhibition (Figures 3E–3G). These experiments reveal that DYRK1A silencing or loss markedly accentuates proliferation induced by the TGFβ inhibitors GW788388 and LY364947, and conversely that DYRK1A overexpression is able to block proliferative effects of the harmine-TGFβ inhibitor combination. Collectively, the studies in Figure 3 illustrate that the majority, if not all, of the synergistic effects of the harmine-TGFβ inhibitor combination on human beta cell proliferation are attributable to combined interruption of both DYRK1A and SMAD signaling. They further reveal that harmine can have unanticipated direct or indirect effects on SMADs to reduce TGFβSF signaling.

The Harmine-TGFβSF Inhibitor Synergy Reflects Complementary Effects on Cyclins/CDKs and CDK Inhibitors

Reasoning that harmine and harmine-TGFβSF inhibitors (and DYRK1A and SMADs, respectively) must ultimately orchestrate cell-cycle entry via cell-cycle activators and cell-cycle inhibitors, we examined gene expression of cell-cycle activators and inhibitors in whole islets treated with vehicle, harmine, TGFβ inhibitor, or the harmine-TGFβ inhibitor combination (Figures 4A and 4B). Harmine alone, as described previously (Wang et al., 2015a), induced expression of a number of cell-cycle activators (e.g., *CDK1*, *CCNA1*, *CCNE2*, and *CDC25A*). In contrast, TGFβ inhibition alone had little effect on cell-cycle activators. Notably, the harmine-TGFβ inhibitor combination induced no further activation of these or other cyclins or cdks: the harmine-TGFβ inhibitor combination was similar to harmine alone. These results were independently confirmed and extended by RNA-seq of human islets (Tables S1 and S2).

Cell-cycle inhibitors behaved differently (Figure 4B). Harmine alone had modest and limited effects on cell-cycle inhibitor expression, with the exception of *CDKN1C* (encoding $p57^{KIP2}$), which declined by ~50% as described previously (Wang et al., 2015a). In contrast, TGFβ inhibition alone, or in combination with harmine, reduced expression of *CDKN2B* (encoding $p15^{INK4b}$), *CDKN1A* (encoding $p21^{CIP}$), and *CDKN1C*/$p57^{KIP2}$. There was also a small but significant reduction in *CDKN2A* (encoding $p16^{INK4a}$). There was no change in the expression of *CDKN1B* (encoding $p27^{CIP}$), an important inhibitor of cell-cycle progression in the mouse beta cell. These results also were independently confirmed and extended by RNA-seq of human islets (Tables S1 and S2).

To explore the mechanism underlying the decline in *CDKN1A*, *CDKN1C*, and *CDKN2B* in response to TGFβ inhibition, we used adenoviruses to silence R-SMADs 2, 3, and 4, or to overexpress I-SMADs 6 and 7 in human islets, and queried effects on *CDKN1A*, *CDKN1C*, and *CDKN2B* expression. Silencing the R-SMADs or overexpressing I-SMADs reduced *CDKN1A* and *CDKN1C* (Figures 4C and 4D), and had a small but non-significant effect on *CDKN2B* (Figure S5A). To determine whether *CDKN1A* and/or *CDKN1C* reductions might underlie the synergistic effects of the TGFβSF inhibition in the harmine-TGFβSF inhibitor combination, we silenced *CDKN1A* and *CDKN1C* in human islets, either alone or in combination with harmine treatment (Figure 4E). As reported previously (Avrahami et al., 2014; Wang et al., 2017), *CDKN1C* silencing led to a modest increase in human beta cell proliferation, whereas silencing *CDKN1A* had no effect. In contrast, in the presence of harmine, silencing of either or both *CDKN1A* and *CDKN1C* led to robust human beta cell proliferation. Finally, to confirm whether or not *CDKN1A*, *CDKN1C*, and *CDKN2B* truly function as cell-cycle inhibitors in human beta cells, we overexpressed them in human islets treated with harmine and the TGFβ inhibitor LY364947. Overexpression of each cell-cycle inhibitor dramatically reduced proliferation in harmine-TGFβ inhibitor-treated human beta cells to rates approaching zero (Figure 4F).

Collectively, these observations suggest a mechanism for the synergistic effects of the harmine-TGFβ inhibitor combination on proliferation: harmine, through DYRK1A inhibition and nuclear NFAT retention (Demozay et al., 2011; Goodyer et al., 2012; Heit et al., 2006; Wang et al., 2015a), and likely other mechanisms discussed below, predominantly activates cell-cycle genes; in a complementary fashion, TGFβ inhibition, via attenuation of SMAD signaling, reduces expression of *CDKN2B*, *CDKN1A*, and *CDKN1C*, each of which normally functions as a cell-cycle inhibitor in human beta cells. This TGFβ inhibitor-mediated reduction in *CDKN2B*, *CDKN1A*, and *CDKN1C* synergizes with the harmine-induced, DYRK1A-mediated increases in cyclins and CDKs, permitting greater cell-cycle activation than occurs via either harmine treatment or TGFβ inhibition alone.

Effects of R-SMADs and Trithorax Complex on Cell-Cycle Inhibitors

R-SMADs may transactivate or repress genes, and may do so in complexes that include Trithorax members (Antebi et al., 2017; Brown and Schneyer, 2010; Brown et al., 2014; Chandrasekharappa et al., 1997; Chen et al., 2009, 2011; Crabtree et al., 2001, 2003; Dhawan et al., 2009, 2016; El-Gohary et al., 2014; Gaarenstroom and Hill, 2014; Macias et al., 2015; Nomura et al., 2014; Smart et al., 2006; Stewart et al., 2015; Xiao et al., 2014, 2016; Zhou et al., 2013). Both Trithorax and SMAD signaling have been implicated in beta cell proliferation in human insulinoma (Wang et al., 2017). Thus, we queried whether R-SMADS 2, 3, and/or 4 might directly interact with regulatory regions of the *CDKN1A* and/or *CDKN1C* genes in human islets

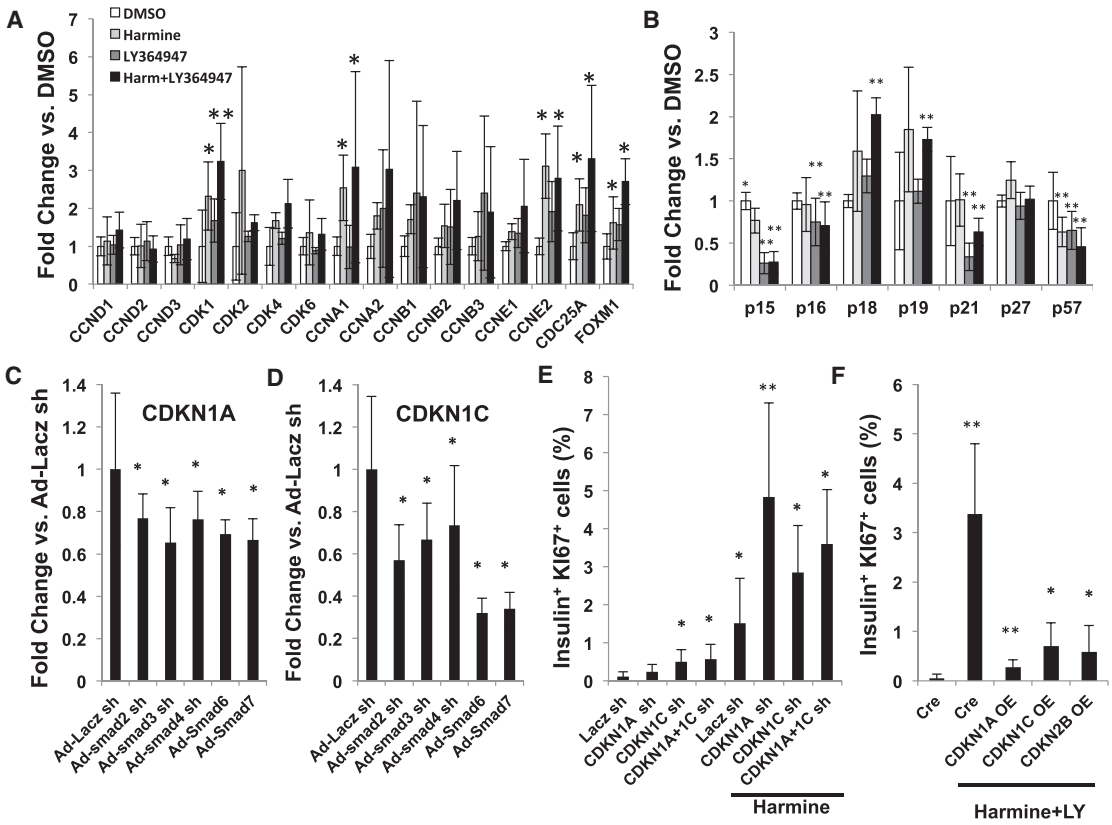

Figure 4. Changes in Cell-Cycle Molecule Expression in Response to Harmine, LY364947, ALK5 Inhibitor, and the Combination

(A) The effects of vehicle (DMSO 0.1%), harmine (10 μM), LY364947 (5 μM), or the combination for 96 hr on gene expression in dispersed human islets for cell-cycle activators, as assessed using qPCR.

(B) Comparable results for cell-cycle inhibitors.

(C and D) The effect of silencing SMADs 2,3,4 or overexpressing SMADs 6 and/or 7 on expression of *CDKN1A* (C) and *CDKN1C* (D) in human islets as assessed using qPCR.

(E) The effects of silencing *CDKN1A*, *CDKN1C*, and the combination on Ki67 immunolabeling in human beta cells in the presence or absence of 10 μM harmine.

(F) The effects of overexpression of *CDKN1A*, *CDKN1C*, and *CDKN2B* in dispersed human islets for 96 hr on proliferation induced by the harmine-LY364947 combination.

All experiments represent five human islet preparations, and error bars represent mean ± SEM. *$p < 0.05$ versus control and **$p < 0.05$ versus harmine. Numbers of donors and beta cells counted are provided in Table S3.

(Figures 5A and 5B). Indeed, SMADs 2/3 and 4 associate with promoter and enhancer regions of *CDKN1A* and *CDKN1C* (black bars in Figures 5C and 5D) defined by Pasquali et al. (2014), and these associations were altered by treatment with the harmine-TGFβ inhibitor combination (white bars). Notably, MEN1, a Trithorax member and H3K4 methylase, was also observed to bind to some of these same regions in *CDKN1A* and *CDKN1C*, and these associations were also altered by harmine-TGFβ inhibitor treatment (Figures 5C and 5D). Finally, the H3K27 demethylase KDM6A, also a Trithorax member that binds specifically to the *CDKN1C* promoter in FACS-sorted human beta cells (Wang et al., 2017), co-localizes with MEN1 on the *CDKN1A* promoter in human islets, and this association is diminished by harmine-TGFβ inhibitor treatment (Figure 5C). Paradoxically, in contrast to results with MEN1, while KDM6A associates with the *CDKN1C* locus in human islets, this association appears to be enhanced rather than reduced with harmine-TGFβ inhibitor treatment (Figure 5D). Taken together, these observations make it clear that R-SMADs, MEN1, and KDM6A do indeed directly or indirectly bind to the regulatory regions of *CDKN1A* and *CDKN1C* in human islets, and do so in regions also occupied by Trithorax members. Importantly, these associations are disrupted by harmine-TGFβ inhibitor treatment. Collectively, these findings are consistent with a model (Figures 5E and 5F) in which SMAD-Trithorax interactions maintain *CDKN1A* and *CDKN1C* expression in beta cells under basal circumstances, under the influence of TGFβSF-mediated SMAD signaling in coordination with a Trithorax-mediated open chromatin state at these loci. Following harmine-TGFβ inhibitor treatment, these complexes appear to dissociate or remodel, apparently disrupting SMAD transactivation of the *CDKN1A* and *CDKN1C* loci.

Combined Harmine-TGFβ Inhibitor Treatment Enhances Mouse and Human Beta Cell Proliferation and Mouse Beta Cell Expansion *In Vivo*

All of the preceding studies were performed in human islets *in vitro*. To determine whether comparable effects could be observed *in vivo*, we employed three models. First, we explored

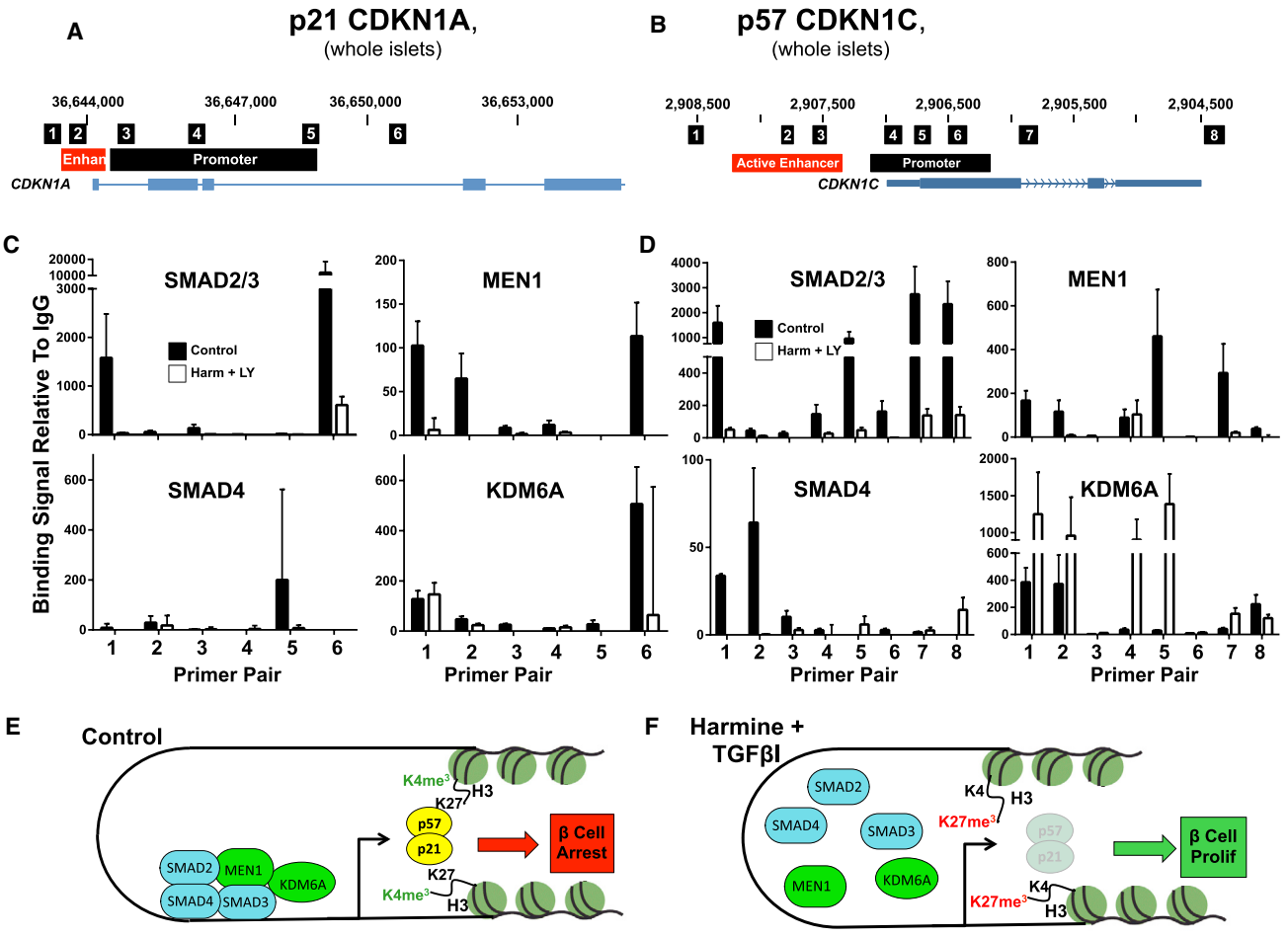

Figure 5. Direct Interaction of SMADs and Trithorax Members with the *CDKN1A* and *CDKN1C* Loci in Human Islets

(A and B) Schematics of the human *CDKN1A* (A) and *CDKN1C* (B) loci from the hg19 UCSC genome browser, showing PCR products amplified in the primer pairs used for ChIP in the small black boxes, the gene bodies in blue below, and enhancers and promoters in orange and black, respectively. Enhancer and promoter loci are derived from Pasquali and Ferrer (Pasquali et al., 2014).

(C and D) ChIP results in control (black bars) and harmine-LY364947-treated (white bars) human islets, with primer pairs corresponding to (A) and (B) along the x axis. Primer pairs and locations for CDKN1A (C) and CDKN1C (D) are derived from Koinuma et al. (2009), Pasquali et al. (2014), and Yang et al. (2009). Experiments were performed on dispersed human islets. Drug treatment lasted for 96 hr. Error bars indicate SEM. Each experiment represents the mean of a minimum of three sets of human islets.

(E and F) Schematics indicating interactions of the SMADs and Trithorax members under basal conditions (E) and following harmine-LY364947 treatment (F), respectively, illustrating that harmine-LY364947 treatment markedly alters SMAD-Trithorax binding to the *CDKN1A* and *CDKN1C* loci. Numbers of donors and beta cells counted are provided in Table S3.

the combined effects of a maximally effective dose of harmine (10 mg/kg i.p. [intraperitoneally]) (Wang et al., 2015a) with ALK5 inhibitor II, SB431542, LY364947, and GW788388, administered once per day for 7 days, on Ki67 beta cell labeling in endogenous pancreatic beta cells of C57BL6 mice. Among these, the combination of harmine (10 mg/kg/day) together with GW788388 (30 mg/kg/day) proved most effective (Figures 6A and 6B), and was selected for subsequent studies. As reported previously, harmine (Wang et al., 2015a) and TGFβSF inhibitors (Dhawan et al., 2016; Xiao et al., 2014; Zhou et al., 2013) individually induce proliferation in mouse beta cells *in vivo*. However, as observed *in vitro*, combined treatment *in vivo* with harmine and GW788388 produced a substantially larger effect than either alone, achieving an *in vivo* beta cell labeling index of 2%.

Second, to determine if the proliferation noted with Ki67 labeling might translate into actual beta cell regeneration *in vivo*, we used the partial (60%) pancreatectomy (PPX) mouse model (Figures 6C, 6D, S5B, and S6) (Wang et al., 2015a). Mice undergoing sham PPX showed no significant change in beta cell mass after 7 days of treatment, although mice treated with the harmine-GW788388 combination appeared to be trending upward. Most importantly, beta cell mass had expanded significantly within 7 days in mice that underwent a 60% PPX followed by the harmine-GW788388 combination. In contrast, the three control groups remained substantially below normal.

Finally, we queried whether systemic treatment with the harmine-GW788388 combination could enhance beta cell proliferation in transplanted human islets *in vivo* in the NOD-SCID mouse

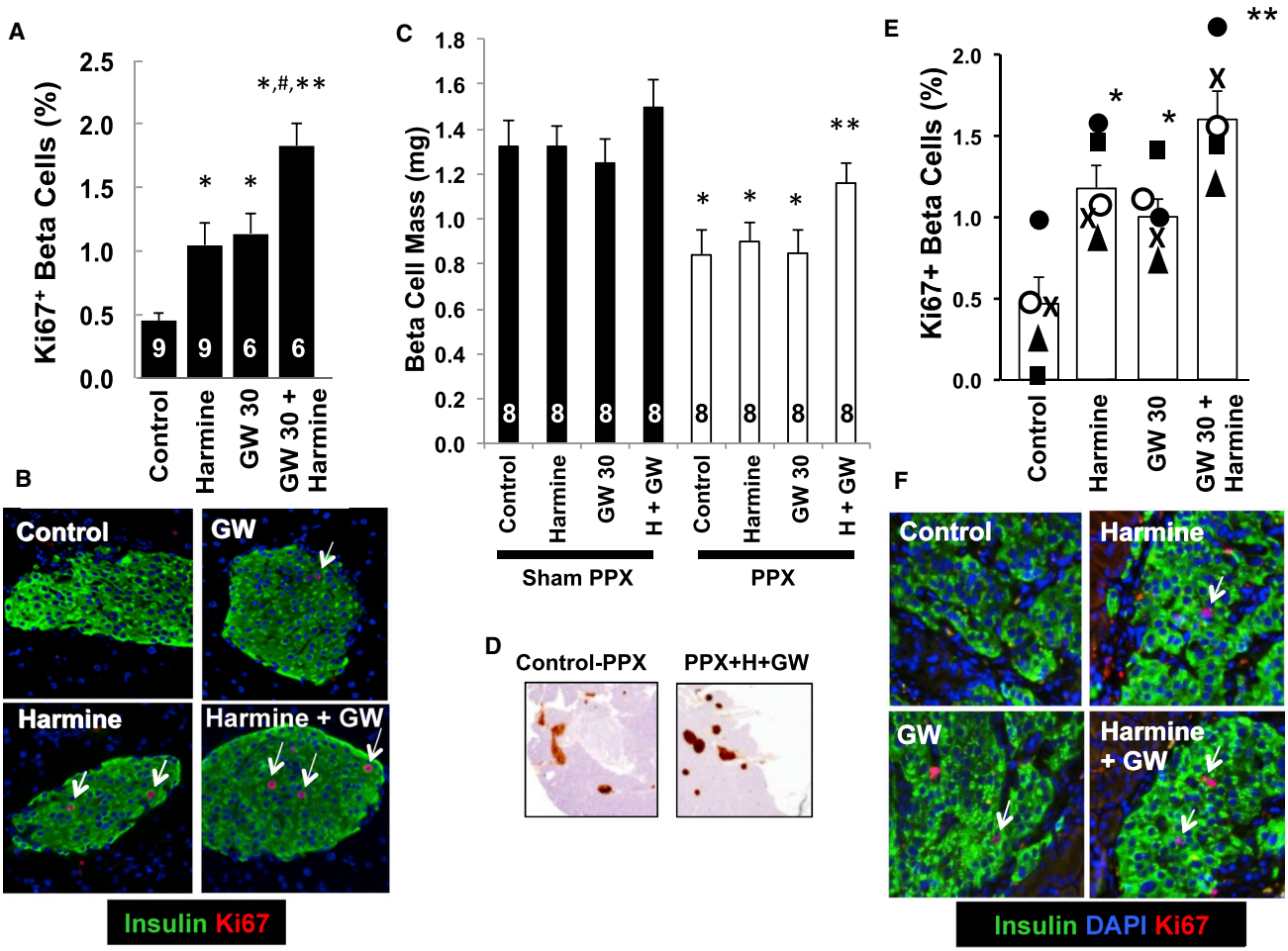

Figure 6. Effects of the Harmine-TGFβ Inhibitor Combination in Three *In Vivo* Models

(A) Intraperitoneal administration of saline (control), 10 mg/kg/day harmine, 30 mg/kg/day GW788388 (GW), or the combination of 10 mg/kg harmine plus 30 mg/kg/day GW788388 daily for 7 days. After 7 days of treatment, the pancreata were harvested and Ki67 and insulin immunolabeling quantified. The numbers of animals in each group are shown within the bars. A minimum of 2,000 beta cells were counted for each bar shown. Error bars indicate SEM. *$p < 0.05$ versus control, #$p < 0.01$ versus harmine or GW alone, and **$p < 0.01$ versus control, by one-way Bonferroni corrected ANOVA.

(B) Examples of Ki67 (red), DAPI (blue), and insulin (green) immunolabeling in each of the four groups in (A). Arrows indicate examples of Ki67$^+$ beta cells.

(C) The effects on total beta cell mass in eight groups of eight C57BL/6N mice receiving daily intraperitoneal vehicle (saline), harmine (10 mg/kg), GW788388 (30 mg/kg), or the harmine-GW788388 combination for 7 days following sham or real 60% pancreatectomy (PPX). Error bars indicate SEM, *$p < 0.05$ versus sham PPX animals, and **$p < 0.05$ versus harmine or GW 30-treated PPX mice.

(D) Examples of pancreas remnants immunolabeled for insulin from mice undergoing PPX treated with control (saline) or the harmine-GW788388 combination. See Figure S6 for details.

(E) The effects of control vehicle (saline), intraperitoneal harmine (10 mg/kg), GW788388 (30 mg/kg), or the harmine-GW788388 combination on human beta cell proliferation for 7 days in five sets of four NOD-SCID mice that received renal capsular islet transplants with 1,000 human islet equivalents from five different islet donors, indicated by the squares, triangles, closed circles, open circles, and "X" symbols. A minimum of 2,000 beta cells were counted for each bar shown. Error bars indicate SEM, *$p < 0.05$ versus control islets, and **$p < 0.05$ versus harmine and GW788388.

(F) Examples of Ki67 (red) and insulin (green) immunolabeling in human islets as in (D). Arrows indicate examples of Ki67$^+$ beta cells.

model (Figures 6E and 6F). As observed previously (Wang et al., 2015a), harmine treatment induced human beta cell proliferation *in vivo*, as did GW788388. Most notably, and as occurred with human beta cells *in vitro* and with mouse beta cells *in vivo*, treatment with the harmine-GW788388 combination was substantially more effective in driving human beta cell proliferation *in vivo* than either agent alone, yielding degrees of beta cell proliferation in transplanted human islets *in vivo* not previously observed by ourselves (Wang et al., 2015a) or others (Dhawan et al., 2016; Dirice et al., 2016) in response to any drug, nutrient, or growth factor. Importantly, beta cells from four of the five islet donors displayed greater Ki67 immunolabeling in the harmine plus GW788388 group than in the three other groups.

DISCUSSION

We provide a number of important new observations. First, we describe a novel combination of two distinct classes of molecules—a DYRK1A inhibitor combined with a TGFβ superfamily inhibitor—that reliably induces "rates" of proliferation in mature

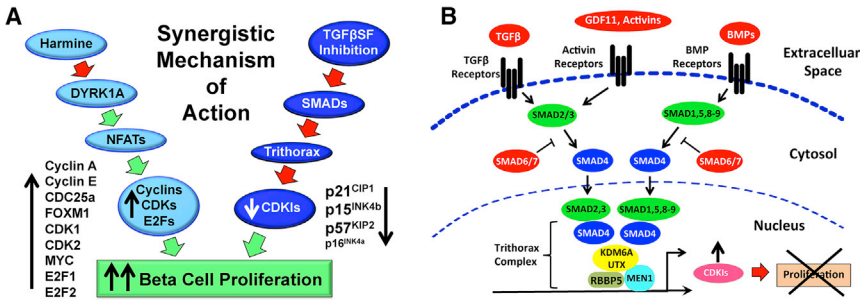

Figure 7. Models of TGFβ Superfamily Signaling and Harmine-TGFβ Superfamily Actions on Human Beta Cell Proliferation

(A) A simplified illustration of the synergistic mechanisms through which harmine and TGFβSF pathway inhibitors cooperate to enhance human beta cell proliferation. Harmine, acting on DYRK1A, primarily activates cyclins, cdks, and related cell-cycle activators. In parallel, TGFβSF pathway inhibitors relieve expression of cell-cycle inhibitors, including *CDKN1A* encoding $p21^{CIP}$, *CDKN1C* encoding $p57^{KIP}$, and *CDKN2B* encoding $p15^{INK4}$. As suggested in Figure 3A, harmine also has direct or indirect effects on TGFβSF-SMAD signaling, and it is likely that DYRK1A has effects on other targets in addition to NFaTs.

(B) In the canonical TGFβ paradigm, ligands such as TGFβ, activins, inhibins, myostatin, GDF11, and bone morphogenic proteins (BMPs) bind to multi-subunit receptors that phosphorylate, and thereby activate, so-called receptor SMADs (SMADs 2,3, and 1,5,8/9). These are then able to heteromerize with SMAD4, a common SMAD, and the SMAD4 heteromers translocate to the nucleus where, among other things, they are incorporated into the chromatin-modifying and DNA-methylating Trithorax complex, and thereby influence expression of multiple gene families. Adapted from Brown and Schneyer (2010).

adult human beta cells averaging 5%–8%, rates not previously been observed with any class of therapeutic molecules, and which far exceed normal physiological pancreatic beta cell replication in the first year of life (Gregg et al., 2012; Kassem et al., 2000; Meier et al., 2008; Wang et al., 2015b). Second, we illustrate that this is a class effect, achieved by many different DYRK1A inhibitors and many different TGFβ superfamily inhibitors. Third, we demonstrate that the DYRK1A inhibitor-TGFβSF inhibitor combination behaves synergistically, and provide novel mechanisms and models for this synergy (Figure 7A). Fourth, we demonstrate that beta cell numbers actually increase in three different models, two human and one murine. Fifth, we provide mechanistic explanations, using both pharmacologic and genetic approaches, for the concept that simultaneous inhibition of DYRK1A and SMAD signaling is both necessary and sufficient for the synergy. Sixth, we document that the beneficial effects on human proliferation are achieved in part via modulation of the activities of chromatin-modifying, epigenetic-modulating enzymes of the Trithorax family, and extend Trithorax beta cell modulatory involvement to KDM6A and likely additional Trithorax members (Figure 7B). Seventh, we observe that beta cell proliferation generated by the harmine-TGFβSF inhibitor combination is not associated with beta cell de-differentiation, and instead favors maintained or increased beta cell differentiation. Eighth, the beneficial mitogenic and pro-differentiation effects of the DYRK1A inhibitor-TGFβSF inhibitor combination extend to beta cells from people with type 2 diabetes. Ninth, we add leucettine-41 (Tahtouh et al., 2012) to the growing list of small-molecule DYRK1A inhibitors that are able to activate human beta cell proliferation. Tenth, we extend the induction of proliferation *in vitro* to three distinct mouse and human *in vivo* models. Eleventh, the observations strongly suggest that locally produced endogenous TGFβSF agonists such as TGFβs activins, inhibins, BMPs, and related molecules play a key physiologic role in restraining beta cell mass expansion, and that this inhibitory pathway can be manipulated for therapeutic purposes. Finally, while DYRK1A remains a central target of harmine and other DYRK1A inhibitors, we suggest that harmine also may act in part via SMAD pathways as well.

While DYRK1A inhibitors such as harmine, 5-IT, INDY, and GNF4877 have been shown to induce replication in human beta cells, the "rates" of proliferation or labeling indices have been low, in the 1.5%–3% range *in vitro* (Aamodt et al., 2016; Abdolazimi et al., 2018; Dirice et al., 2016; Shen et al., 2015; Wang et al., 2015a, 2016), and far lower in *in vivo* transplant models (Dirice et al., 2016; Wang et al., 2015a). Thus, while harmine analog-induced beta cell proliferation is an important advance, one might envision higher rates of proliferation as being required for therapeutic human beta cell expansion in type 1 and type 2 diabetes. The average "rates" in the 5%–8% range obtained with the DYRK1A inhibitor-TGFβ inhibitor combination (Figures 1 and 2) are notable in this regard.

TGFβ inhibitors and SMAD inhibition are well known as activators of proliferation in rodent islets (Brown and Schneyer, 2010; Brown et al., 2014; Dhawan et al., 2016; El-Gohary et al., 2014; Mukherjee et al., 2007; Nomura et al., 2014; Smart et al., 2006; Xiao et al., 2014, 2016; Zhou et al., 2013). For example, Schneyer et al. demonstrated in 2007 that knockout of the endogenous activin inhibitor follistatin-like-3 leads to beta cell expansion in mouse genetic models (Mukherjee et al., 2007). Teramoto et al. have reported that beta cell-specific disruption of *smad2* leads to beta cell hyperplasia (Nomura et al., 2014). Kim and Gittes have both reported that spontaneous or inducible upregulation of the I-SMAD *smad7* is associated with beta cell proliferation and expansion in mice (Smart et al., 2006; Xiao et al., 2014, 2016). And Bhushan, Kulkarni et al. have used small-molecule TGFβ receptor inhibitors to activate proliferation in mouse pancreatic beta cells (Dhawan et al., 2016; Zhou et al., 2013). When examined in adult human islets, however, beta cell proliferation in response to TGFβSF inhibitors has been modest or negligible (Dhawan et al., 2016), a result we confirm (Figure 1A).

One important advance herein was to employ TGFβ inhibitors in combination with harmine, a concept we derived from human insulinoma data mining, wherein both DYRK1A and SMAD pathway abnormalities are evident (Wang et al., 2017). Moreover, we observe that inhibiting many of the various classes of TGFβ superfamily receptors, including TGFβ, activin, and BMP receptors, in the presence of harmine, is effective in permitting beta cell proliferation. We also find, as reported previously (Brown et al., 2014), that TGFβ superfamily members and SMAD signaling pathways are abundant in human islets. We infer that these collectively comprise an inhibitory regulatory network that restrains human beta cell proliferation, perhaps, as suggested by Gittes and Kim, to protect against de-differentiation

(Smart et al., 2006; Xiao et al., 2014, 2016), or perhaps against inappropriate beta cell expansion that might cause dangerous hypoglycemia, as occurs in insulinoma and congenital hyperinsulinism. Importantly, the efficacy of the harmine-TGFβSF inhibitor combination translates from purely *in vitro* systems to three different *in vivo* models.

Another key advance is the demonstration that the increases in beta cell proliferation implied by elevated Ki67, BrdU, and pHH3 labeling measures widely used in beta cell biology actually translate into increases in numbers of human beta cells. It has been challenging to demonstrate actual increases in human beta cell numbers in response to any agent. Laffitte observed an increase in human beta cell numbers *in vitro* in response to GNF4877 using advanced imaging techniques (Shen et al., 2015). Fiaschi-Taesch, using complex imaging and image analysis, also showed that cyclin and cyclin-dependent kinase overexpression using gene therapy approaches was able to increase human beta cell numbers (Tiwari et al., 2015). And Kerr-Conte et al. suggested that transplanted human islet cell mass can increase in response to high-fat feeding (Gargani et al., 2013). Each of these models is tedious and/or requires advanced imaging equipment, barriers to their widespread adoption. Not surprisingly, therefore, none of these approaches has been widely adopted. Here, we report a straightforward flow cytometric method to assess actual human beta cell numbers, and demonstrate its ease and efficacy in two different human beta cell models. Using this method, we find that adult beta cell numbers are approximately 50% higher in human islets treated for 4 days with the harmine-TGFβ inhibitor combination than control islets (Figure 1H). This is in the general range that might be anticipated with a proliferation rate of 5%–8%. For example, one might predict conservatively that a labeling index of 5%–8%/day over 4 days would lead to a 22%–36% increase in beta cell numbers. Along the same lines, in the Mel1-hESC experiments, which continued for 7 days, one might assume a 50%–70% increase in beta cell numbers, approximating the near doubling observed (Figure 1I). Of course, these calculations are approximate and rely on imperfect assumptions, but may suggest that the Ki67 labeling indices actually underestimate the true rate of beta cell proliferation. Thus, alternately or in addition, they may reflect additional beneficial effects on beta cell survival, on enhanced beta cell differentiation, and/or on transdifferentiation from other islet cell types. Whatever the mechanisms, increases in human beta cell numbers of this magnitude following 4–7 days of treatment would be a welcome addition to the regenerative armamentarium.

We find that the DYRK1A inhibitor-TGFβSF inhibitor combination is not merely additive, but clearly synergistic (Figures 1, S1A, and S1B). Mechanistically, DYRK1A inhibitors seem to preferentially activate cell-cycle activators, such as cyclins and cdks, whereas the TGFβSF inhibitors seem to preferentially repress cell-cycle inhibitors, notably *CDKN1A*, *CDKN1C*, and *CDKN2B*, effects that appear to be mediated, at least for *CDKN1A* and *CDKN1C*, by SMAD signaling and Trithorax chromatin remodeling. While we find clear evidence for TGFβ superfamily member effects being mediated by *CDKN1A* and *CDKN1C*, documenting involvement of *CDKN2B* and *CDKN2A* is more difficult because they arise from a common locus that encodes additional cell-cycle modulators such as $p14^{ARF}$, ANRIL, and others. These issues, and the unusually GC-rich nature of this locus, make selective silencing of *CDKN2A* and *CDKN2B* challenging. Finally, while the apparent complementary actions of DYRK1A inhibitors and TGFβ superfamily inhibitors, illustrated in Figure 7A, likely explain much of the apparent synergy, they are unlikely the exclusive mechanism for the observed synergy, as evidenced by the ability of harmine alone to modulate expression and abundance of TGFβ superfamily members (Figure 3A; Table S2). Indeed, several reports indicate that DYRK1A can phosphorylate a broad range of targets in addition to the NFaT family, including Tau, TP53, $p27^{CIP}$, and the DREAM complex member LIN52 (Abdolazimi et al., 2018; Branca et al., 2017; Litovchick et al., 2011; Park et al., 2010; Sadasivam and DeCaprio, 2013). We thus speculate that currently unknown additional targets likely exist that may lead to destabilization and/or dephosphorylation of SMADs as observed in Figure 3A. Clarification of these additional mechanisms in future studies is warranted.

The involvement of the Trithorax family of epigenetic modifying genes in controlling beta cell growth is not unexpected. The canonical Trithorax member *MEN1* was positionally cloned from people with the multiple endocrine neoplasia type 1 syndrome (Chandrasekharappa et al., 1997), which includes insulinomas. MEN1 and other Trithorax members have been shown to regulate beta cell proliferation and mass in animal models and cell lines (Crabtree et al., 2001, 2003; Dhawan et al., 2016; Karnik et al., 2005; Zhou et al., 2013). Moreover, MEN1 and other Trithorax members, such as MLLs, have also been shown to participate in rodent beta cell proliferation and directly bind using chromatin immunoprecipitation (ChIP) to cell-cycle inhibitor loci (Dhawan et al., 2016; Zhou et al., 2013). In addition, another Trithorax member, KDM6A, has recently been shown to be recurrently inactivated in human insulinomas (Wang et al., 2017); silencing or pharmacologically inhibiting KDM6A in human beta cells can block expression of the cell-cycle inhibitor *CDKN1C* (Wang et al., 2017). Here, we extend these observations by showing that the DYRK1A inhibitor-TGFβSF inhibitor combination disrupts normal physical interactions among MEN1 and KDM6A with *CDKN1A* and *CDKN1C* promoters and enhancers, and provide for the first time an example of harmine-TGFβSF inhibition modulating the binding of the canonical Trithorax member MEN1 to regulatory regions of the key cell-cycle inhibitor *CDKN1C* in human islets. Since these studies were performed in whole islets, additional studies will be required to elucidate which events actually occur in beta cells. Similarly, genome-wide studies such as ChIP-seq and ATAC-seq using purified beta cells will be required to document and clarify specific interactions on a genome-wide basis.

Accili and collaborators have reported that type 2 diabetes in mouse and human beta cells is associated with de-differentiation to a more primitive, and poorly functional, insulin-depleted neuroendocrine cell type (Talchai et al., 2012). As was the case with harmine (Wang et al., 2015a), the harmine-TGFβSF inhibitor combination increased several key markers of human beta cell identity, differentiation, and maturity, including *NKX6.1*, *PDX1*, *MAFA*, *MAFB*, *SLC2A2*, and *PCSK1* (Figures 2A–2C; Table S2). We presume, but have not experimentally confirmed, that this relates in part to DYRK1A inhibition with resultant NFaT nuclear translocation and binding to promoters of this class of genes, as documented by Kim et al. in mouse beta cells

(Goodyer et al., 2012; Heit et al., 2006). The observation that some, but not all, presumptive beta cell differentiation factors are increased in human islets treated with the harmine-TGFβ inhibitor combination is reminiscent of observations of Sekine et al. (1994) and Klochendler et al. (2016), who observed that proliferating Ins1 cells (Sekine et al., 1994) or mouse beta cells (Klochendler et al., 2016) display varying effects on key beta cell functions, such as reducing lactate dehydrogenase (LDH) activity, and on transcriptomic readouts. For example, abundance of mRNAs encoding the key beta cell transcription factors *Nkx6.1*, *Mafa*, and *Pdx1* remained normal in proliferating mouse beta cells, while transcripts encoding genes involved in secretory granule function such as secretogranin V (Scg5), Pcsk1, Vamp4, carboxypeptidase (Cpe), and Rab3a were reduced. Clarifying such complex events will require studies in single cells, at multiple time points, and in response to multiple treatments, and in islets from normals and people with type 2 diabetes, employing technologies such as single-cell RNA-seq, CyTOF analysis, and microsecretion studies from individual beta cells. From a therapeutic standpoint, the fact that a differentiated molecular phenotype and glucose-stimulated insulin secretion remain intact despite induction of proliferation in normal (Figures 2A–2D) and type 2 diabetes islets (Figures 2E and 2F) bodes well for treatment of people with type 2 diabetes, and merits further exploration.

Limitations of Study

A number of important additional challenges remain in the field of beta cell regenerative research. First, this study employed islets from 104 different human islet donors, illustrating a major challenge the field of regenerative beta cell biology faces. The field lacks easy and affordable access to large numbers of human islets, which themselves are remarkably heterogeneous; unequivocal, universally accepted approaches to high-throughput, high-precision human cadaveric beta cell drug screening and quantitation; and perfect model cell lines with which to perform such studies.

Second, beta cell targeting remains a major challenge. Since SMAD and DYRK1A signaling are ubiquitous, the DYRK1A inhibitor-TGFβSF inhibitor strategy will certainly have off-target effects on many tissues, as illustrated by the CNS effects of harmine (Brierley and Davidson, 2012; Heise and Brooks, 2017) and the mitogenic effects of the harmine-TGFβSF inhibitor effects on alpha and ductal cells (Figure S3). At this moment, there is no molecule that is able to target or deliver any drug specifically to the beta cell, an observation that has prompted urgent requests for such targeting molecules from diabetes funding agencies. Thus, one might envision a future in which drugs such as harmine and TGFβ inhibitors might be administered systemically and delivered directly and specifically to human beta cells—but not to other cell types—via carrier or transport molecules such as beta cell-specific GLP1 analogs, monoclonal antibodies, RNA aptamers, and/or zincophilic delivery molecules. Alternately, one might imagine using the drug combination to expand human islets *ex vivo* prior to transplantation.

A third concern relates to the potential long-term effect of TGFβSF inhibitors to cause de-differentiation in beta cells. Both Gittes and Kim have reported in mouse models that upregulation or overexpression of the I-SMAD *smad7* in beta cells over the longer term results in beta cell de-differentiation, but that re-differentiation occurs in association with termination of the SMAD7 signal (Smart et al., 2006; Xiao et al., 2014, 2016). Teramoto et al. report that knockout of the R-SMAD *smad2* also induces beta cell de-differentiation (Nomura et al., 2014). These observations predict that continuous long-term TGFβSF inhibition may result in human beta cell de-differentiation, and that cyclical dosing strategies may be required, as is commonly employed with TGFβSF inhibitors in current clinical use (Cohn et al., 2014; Herbertz et al., 2015; Mascarenhas et al., 2014; Necchi et al., 2014; Trachtman et al., 2011; Yanagita, 2012). A fourth challenge is that proliferation rates appear less robust *in vivo* (~2%) than *in vitro* (~5%–8%), a result that we speculate reflects the greater abundance of TGFβSF ligands in the *in vivo* environment versus *in vitro*. Of particular relevance here is the observation that although the TGFβ inhibitor GW788388 had no mitogenic effect on human beta cells *in vitro* (Figure 1A), it did increase proliferation *in vivo* (Figures 6E and 6F). This may provide additional support for the concept that endogenous TGFβSF ligands serve as important *in vivo* physiologic repressors of adult human beta cell replication.

Finally, while these strategies appear to be promising for both type 1 and type 2 diabetes, they may be particularly attractive in type 2 diabetes, since residual beta cell mass is substantially higher in type 2 than in type 1 diabetes, and since autoimmunity is not operative. Most important, these studies support the possibility that restorative treatment of beta cell deficiency and function in type 1 and type 2 diabetes is achievable.

STAR★METHODS

Detailed methods are provided in the online version of this paper and include the following:

- KEY RESOURCES TABLE
- CONTACT FOR REAGENT AND RESOURCE SHARING
- EXPERIMENTAL MODEL AND SUBJECT DETAILS
  - Human Pancreatic Islet Studies
  - Mouse Studies
- METHOD DETAILS
  - Adenoviruses and Transduction
  - Quantitative PCR
  - RNA sequencing
  - Immunocytochemistry
  - Immunoblotting
  - Glucose-Stimulated Insulin Secretion
  - Proliferation in HUES8-Derived Human Beta Cells
  - Expansion and Differentiation of Mel1-Derived Beta Cells: Stem cell line and culture
  - Differentiation of Mel1 Cells into Pancreatic Islets
  - Flow Cytometry to Quantify Human Beta Cells
  - Chromatin Immunoprecipitation (ChIP) Assays
- QUANTIFICATION AND STATISTICAL ANALYSIS
  - Statistics
- DATA AND SOFTWARE AVAILIBILITY

SUPPLEMENTAL INFORMATION

Supplemental Information includes seven figures and three tables and can be found with this article online at https://doi.org/10.1016/j.cmet.2018.12.005.

ACKNOWLEDGMENTS

The authors wish to thank Bonnie and Joel Bergstein and Thomas and Lonnie Schwartz for their support of this project. We thank NIDDK Integrated Islet Distribution Program (IIDP), Dr. Tatsuya Kin at the University of Edmonton, and Dr. Patrick MacDonald at the Alberta Diabetes Institute for supplying human cadaveric islets, and The Human Islet and Adenoviral Core (HIAC) of the Einstein-Sinai Diabetes Research Center (DRC) at the Icahn School of Medicine at Mount Sinai for support in developing the many human adenoviruses described in this project. We thank Dr. Martin Walsh for advice with ChIP studies. We also thank the Genomics and Flow Cytometry Cores at the Icahn School of Medicine at Mount Sinai. This work was supported by seed funding from the Icahn School of Medicine at Mount Sinai; by NIDDK grants R-01 DK 105015, R01 DK108905, UC4 DK104211, P-30 DK 020541, and R-01 DK116873; by JDRF grant 2-SRA-2017 514-S-B; and by ADA grant 1-16-ICTS-029.

AUTHOR CONTRIBUTIONS

P.W., E.K., H.L., E.S., C. Ackeifi, B.J.G., V.Z., A.B., K.K.T., L.Y., J.W., and A.G.-O. performed experiments. P.W. and A.F.S. conceived of the overall strategy. P.W., E.K., D.K.S., D.H., D.E., G.H., F.P., C. Argmann, A.G.-O., and A.F.S. analyzed and interpreted data. P.W., E.K., G.H., D.K.S., A.G.-O. and A.F.S. wrote the manuscript.

DECLARATIONS OF INTEREST

A.F.S. and P.W. are inventors on a patent that has been filed by the Icahn School of Medicine at Mount Sinai. G.H., L.Y., and F.P. are employees of Semma Therapeutics.

Received: March 20, 2018
Revised: August 3, 2018
Accepted: November 30, 2018
Published: December 20, 2018

REFERENCES

Aamodt, K.I., Aramandla, R., Brown, J.J., Fiaschi-Taesch, N., Wang, P., Stewart, A.F., Brissova, M., and Powers, A.C. (2016). Development of a reliable automated screening system to identify small molecules and biologics that promote human β-cell regeneration. Am. J. Physiol. Endocrinol. Metab. *311*, E859–E868.

Abdolazimi, Y., Zhao, Z., Lee, S., Xu, H., Allegretti, P., Horton, T.M., Yeh, B., Moeller, H.P., Nichols, R.J., McCutcheon, D., et al. (2018). CC-401 promotes β-cell replication via pleiotropic consequences of DYRK1A/B inhibition. Endocrinology *159*, 3143–3157.

Antebi, Y.E., Linton, J.M., Klumpe, H., Bintu, B., Gong, M., Su, C., McCardell, R., and Elowitz, M.B. (2017). Combinatorial signal perception in the BMP pathway. Cell *170*, 1184–1196.e24.

Avrahami, D., Li, C., Yu, M., Jiao, Y., Zhang, J., Naji, A., Ziaie, S., Glaser, B., and Kaestner, K.H. (2014). Targeting the cell cycle inhibitor p57Kip2 promotes adult human β cell replication. J. Clin. Invest. *124*, 670–674.

Branca, C., Shaw, D.M., Belfiore, R., Gokhale, V., Shaw, A.Y., Foley, C., Smith, B., Hulme, C., Dunckley, T., Meechoovet, B., et al. (2017). Dyrk1 inhibition improves Alzheimer's disease-like pathology. Aging Cell *16*, 1146–1154.

Brierley, D.I., and Davidson, C. (2012). Developments in harmine pharmacology–implications for ayahuasca use and drug-dependence treatment. Prog. Neuropsychopharmacol. Biol. Psychiatry *39*, 263–272.

Brown, M.L., and Schneyer, A.L. (2010). Emerging roles for the TGFbeta family in pancreatic beta-cell homeostasis. Trends Endocrinol. Metab. *21*, 441–448.

Brown, M.L., Ungerleider, N., Bonomi, L., Andrzejewski, D., Burnside, A., and Schneyer, A. (2014). Effects of activin A on survival, function and gene expression of pancreatic islets from non-diabetic and diabetic human donors. Islets *6*, e1017226.

Chandrasekharappa, S.C., Guru, S.C., Manickam, P., Olufemi, S.E., Collins, F.S., Emmert-Buck, M.R., Debelenko, L.V., Zhuang, Z., Lubensky, I.A., Liotta, L.A., et al. (1997). Positional cloning of the gene for multiple endocrine neoplasia-type 1. Science *276*, 404–407.

Chen, H., Gu, X., Su, I.H., Bottino, R., Contreras, J.L., Tarakhovsky, A., and Kim, S.K. (2009). Polycomb protein Ezh2 regulates pancreatic beta-cell Ink4a/Arf expression and regeneration in diabetes mellitus. Genes Dev. *23*, 975–985.

Chen, H., Gu, X., Liu, Y., Wang, J., Wirt, S.E., Bottino, R., Schorle, H., Sage, J., and Kim, S.K. (2011). PDGF signalling controls age-dependent proliferation in pancreatic β-cells. Nature *478*, 349–355.

Cinti, F., Bouchi, R., Kim-Muller, J.Y., Ohmura, Y., Sandoval, P.R., Masini, M., Marselli, L., Suleiman, M., Ratner, L.E., Marchetti, P., and Accili, D. (2016). Evidence of β-cell dedifferentiation in human type 2 diabetes. J. Clin. Endocrinol. Metab. *101*, 1044–1054.

Cohn, A., Lahn, M.M., Williams, K.E., Cleverly, A.L., Pitou, C., Kadam, S.K., Farmen, M.W., Desaiah, D., Raju, R., Conkling, P., and Richards, D. (2014). A phase I dose-escalation study to a predefined dose of a transforming growth factor-β1 monoclonal antibody (TβM1) in patients with metastatic cancer. Int. J. Oncol. *45*, 2221–2231.

Cozar-Castellano, I., Takane, K.K., Bottino, R., Balamurugan, A.N., and Stewart, A.F. (2004). Induction of beta-cell proliferation and retinoblastoma protein phosphorylation in rat and human islets using adenovirus-mediated transfer of cyclin-dependent kinase-4 and cyclin D1. Diabetes *53*, 149–159.

Crabtree, J.S., Scacheri, P.C., Ward, J.M., Garrett-Beal, L., Emmert-Buck, M.R., Edgemon, K.A., Lorang, D., Libutti, S.K., Chandrasekharappa, S.C., Marx, S.J., et al. (2001). A mouse model of multiple endocrine neoplasia, type 1, develops multiple endocrine tumors. Proc. Natl. Acad. Sci. USA *98*, 1118–1123.

Crabtree, J.S., Scacheri, P.C., Ward, J.M., McNally, S.R., Swain, G.P., Montagna, C., Hager, J.H., Hanahan, D., Edlund, H., Magnuson, M.A., et al. (2003). Of mice and MEN1: insulinomas in a conditional mouse knockout. Mol. Cell. Biol. *23*, 6075–6085.

Demozay, D., Tsunekawa, S., Briaud, I., Shah, R., and Rhodes, C.J. (2011). Specific glucose-induced control of insulin receptor substrate-2 expression is mediated via Ca2+-dependent calcineurin/NFAT signaling in primary pancreatic islet β-cells. Diabetes *60*, 2892–2902.

Dhawan, S., Tschen, S.I., and Bhushan, A. (2009). Bmi-1 regulates the Ink4a/Arf locus to control pancreatic beta-cell proliferation. Genes Dev. *23*, 906–911.

Dhawan, S., Dirice, E., Kulkarni, R.N., and Bhushan, A. (2016). Inhibition of TGF-β signaling promotes human pancreatic β-cell replication. Diabetes *65*, 1208–1218.

Dirice, E., Walpita, D., Vetere, A., Meier, B.C., Kahraman, S., Hu, J., Dančík, V., Burns, S.M., Gilbert, T.J., Olson, D.E., et al. (2016). Inhibition of DYRK1A stimulates human β-cell proliferation. Diabetes *65*, 1660–1671.

El-Gohary, Y., Tulachan, S., Wiersch, J., Guo, P., Welsh, C., Prasadan, K., Paredes, J., Shiota, C., Xiao, X., Wada, Y., et al. (2014). A smad signaling network regulates islet cell proliferation. Diabetes *63*, 224–236.

Fiaschi-Taesch, N., Bigatel, T.A., Sicari, B., Takane, K.K., Salim, F., Velazquez-Garcia, S., Harb, G., Selk, K., Cozar-Castellano, I., and Stewart, A.F. (2009). Survey of the human pancreatic beta-cell G1/S proteome reveals a potential therapeutic role for cdk-6 and cyclin D1 in enhancing human beta-cell replication and function in vivo. Diabetes *58*, 882–893.

Fiaschi-Taesch, N.M., Kleinberger, J.W., Salim, F.G., Troxell, R., Wills, R., Tanwir, M., Casinelli, G., Cox, A.E., Takane, K.K., Scott, D.K., and Stewart, A.F. (2013a). Human pancreatic β-cell G1/S molecule cell cycle atlas. Diabetes *62*, 2450–2459.

Fiaschi-Taesch, N.M., Kleinberger, J.W., Salim, F.G., Troxell, R., Wills, R., Tanwir, M., Casinelli, G., Cox, A.E., Takane, K.K., Srinivas, H., et al. (2013b). Cytoplasmic-nuclear trafficking of G1/S cell cycle molecules and adult human β-cell replication: a revised model of human β-cell G1/S control. Diabetes *62*, 2460–2470.

Gaarenstroom, T., and Hill, C.S. (2014). TGF-β signaling to chromatin: how Smads regulate transcription during self-renewal and differentiation. Semin. Cell Dev. Biol. *32*, 107–118.

Gargani, S., Thévenet, J., Yuan, J.E., Lefebvre, B., Delalleau, N., Gmyr, V., Hubert, T., Duhamel, A., Pattou, F., and Kerr-Conte, J. (2013). Adaptive changes of human islets to an obesogenic environment in the mouse. Diabetologia *56*, 350–358.

Goodyer, W.R., Gu, X., Liu, Y., Bottino, R., Crabtree, G.R., and Kim, S.K. (2012). Neonatal β cell development in mice and humans is regulated by calcineurin/NFAT. Dev. Cell *23*, 21–34.

Gregg, B.E., Moore, P.C., Demozay, D., Hall, B.A., Li, M., Husain, A., Wright, A.J., Atkinson, M.A., and Rhodes, C.J. (2012). Formation of a human β-cell population within pancreatic islets is set early in life. J. Clin. Endocrinol. Metab. *97*, 3197–3206.

Heise, C.W., and Brooks, D.E. (2017). Ayahuasca exposure: descriptive analysis of calls to US Poison Control Centers from 2005 to 2015. J. Med. Toxicol. *13*, 245–248.

Heit, J.J., Apelqvist, A.A., Gu, X., Winslow, M.M., Neilson, J.R., Crabtree, G.R., and Kim, S.K. (2006). Calcineurin/NFAT signalling regulates pancreatic beta-cell growth and function. Nature *443*, 345–349.

Herbertz, S., Sawyer, J.S., Stauber, A.J., Gueorguieva, I., Driscoll, K.E., Estrem, S.T., Cleverly, A.L., Desaiah, D., Guba, S.C., Benhadji, K.A., et al. (2015). Clinical development of galunisertib (LY2157299 monohydrate), a small molecule inhibitor of transforming growth factor-beta signaling pathway. Drug Des. Devel. Ther. *9*, 4479–4499.

Karnik, S.K., Hughes, C.M., Gu, X., Rozenblatt-Rosen, O., McLean, G.W., Xiong, Y., Meyerson, M., and Kim, S.K. (2005). Menin regulates pancreatic islet growth by promoting histone methylation and expression of genes encoding p27Kip1 and p18INK4c. Proc. Natl. Acad. Sci. USA *102*, 14659–14664.

Kassem, S.A., Ariel, I., Thornton, P.S., Scheimberg, I., and Glaser, B. (2000). Beta-cell proliferation and apoptosis in the developing normal human pancreas and in hyperinsulinism of infancy. Diabetes *49*, 1325–1333.

Klochendler, A., Caspi, I., Corem, N., Moran, M., Friedlich, O., Elgavish, S., Nevo, Y., Helman, A., Glaser, B., Eden, A., et al. (2016). The genetic program of pancreatic β-cell replication in vivo. Diabetes *65*, 2081–2093.

Koinuma, D., Tsutsumi, S., Kamimura, N., Imamura, T., Aburatani, H., and Miyazono, K. (2009). Promoter-wide analysis of Smad4 binding sites in human epithelial cells. Cancer Sci. *100*, 2133–2142.

Litovchick, L., Florens, L.A., Swanson, S.K., Washburn, M.P., and DeCaprio, J.A. (2011). DYRK1A protein kinase promotes quiescence and senescence through DREAM complex assembly. Genes Dev. *25*, 801–813.

Macias, M.J., Martin-Malpartida, P., and Massagué, J. (2015). Structural determinants of Smad function in TGF-β signaling. Trends Biochem. Sci. *40*, 296–308.

Mascarenhas, J., Li, T., Sandy, L., Newsom, C., Petersen, B., Godbold, J., and Hoffman, R. (2014). Anti-transforming growth factor-β therapy in patients with myelofibrosis. Leuk. Lymphoma *55*, 450–452.

Meier, J.J., Butler, A.E., Saisho, Y., Monchamp, T., Galasso, R., Bhushan, A., Rizza, R.A., and Butler, P.C. (2008). Beta-cell replication is the primary mechanism subserving the postnatal expansion of beta-cell mass in humans. Diabetes *57*, 1584–1594.

Micallef, S.J., Li, X., Schiesser, J.V., Hirst, C.E., Yu, Q.C., Lim, S.M., Nostro, M.C., Elliott, D.A., Sarangi, F., Harrison, L.C., et al. (2012). INS(GFP/w) human embryonic stem cells facilitate isolation of in vitro derived insulin-producing cells. Diabetologia *55*, 694–706.

Millman, J.R., Xie, C., Van Dervort, A., Gürtler, M., Pagliuca, F.W., and Melton, D.A. (2016). Generation of stem cell-derived β-cells from patients with type 1 diabetes. Nat. Commun. *7*, 11463.

Mukherjee, A., Sidis, Y., Mahan, A., Raher, M.J., Xia, Y., Rosen, E.D., Bloch, K.D., Thomas, M.K., and Schneyer, A.L. (2007). FSTL3 deletion reveals roles for TGF-beta family ligands in glucose and fat homeostasis in adults. Proc. Natl. Acad. Sci. USA *104*, 1348–1353.

Necchi, A., Giannatempo, P., Mariani, L., Farè, E., Raggi, D., Pennati, M., Zaffaroni, N., Crippa, F., Marchianò, A., Nicolai, N., et al. (2014). PF-03446962, a fully-human monoclonal antibody against transforming growth-factor β (TGFβ) receptor ALK1, in pre-treated patients with urothelial cancer: an open label, single-group, phase 2 trial. Invest. New Drugs *32*, 555–560.

Nomura, M., Zhu, H.L., Wang, L., Morinaga, H., Takayanagi, R., and Teramoto, N. (2014). SMAD2 disruption in mouse pancreatic beta cells leads to islet hyperplasia and impaired insulin secretion due to the attenuation of ATP-sensitive K+ channel activity. Diabetologia *57*, 157–166.

Pagliuca, F.W., Millman, J.R., Gürtler, M., Segel, M., Van Dervort, A., Ryu, J.H., Peterson, Q.P., Greiner, D., and Melton, D.A. (2014). Generation of functional human pancreatic β cells in vitro. Cell *159*, 428–439.

Park, J., Oh, Y., Yoo, L., Jung, M.S., Song, W.J., Lee, S.H., Seo, H., and Chung, K.C. (2010). Dyrk1A phosphorylates p53 and inhibits proliferation of embryonic neuronal cells. J. Biol. Chem. *285*, 31895–31906.

Pasquali, L., Gaulton, K.J., Rodríguez-Seguí, S.A., Mularoni, L., Miguel-Escalada, I., Akerman, İ., Tena, J.J., Morán, I., Gómez-Marín, C., van de Bunt, M., et al. (2014). Pancreatic islet enhancer clusters enriched in type 2 diabetes risk-associated variants. Nat. Genet. *46*, 136–143.

Pullen, T.J., and Rutter, G.A. (2013). When less is more: the forbidden fruits of gene repression in the adult β-cell. Diabetes Obes. Metab. *15*, 503–512.

Sadasivam, S., and DeCaprio, J.A. (2013). The DREAM complex: master coordinator of cell cycle-dependent gene expression. Nat. Rev. Cancer *13*, 585–595.

Schuit, F., Van Lommel, L., Granvik, M., Goyvaerts, L., de Faudeur, G., Schraenen, A., and Lemaire, K. (2012). β-cell-specific gene repression: a mechanism to protect against inappropriate or maladjusted insulin secretion? Diabetes *61*, 969–975.

Sekine, N., Cirulli, V., Regazzi, R., Brown, L.J., Gine, E., Tamarit-Rodriguez, J., Girotti, M., Marie, S., MacDonald, M.J., Wollheim, C.B., et al. (1994). Low lactate dehydrogenase and high mitochondrial glycerol phosphate dehydrogenase in pancreatic beta-cells. Potential role in nutrient sensing. J. Biol. Chem. *269*, 4895–4902.

Shen, W., Taylor, B., Jin, Q., Nguyen-Tran, V., Meeusen, S., Zhang, Y.Q., Kamireddy, A., Swafford, A., Powers, A.F., Walker, J., et al. (2015). Inhibition of DYRK1A and GSK3B induces human β-cell proliferation. Nat. Commun. *6*, 8372.

Smart, N.G., Apelqvist, A.A., Gu, X., Harmon, E.B., Topper, J.N., MacDonald, R.J., and Kim, S.K. (2006). Conditional expression of Smad7 in pancreatic beta cells disrupts TGF-beta signaling and induces reversible diabetes mellitus. PLoS Biol. *4*, e39.

Stewart, A.F., Hussain, M.A., García-Ocaña, A., Vasavada, R.C., Bhushan, A., Bernal-Mizrachi, E., and Kulkarni, R.N. (2015). Human β-cell proliferation and intracellular signaling: part 3. Diabetes *64*, 1872–1885.

Sui, L., Danzl, N., Campbell, S.R., Viola, R., Williams, D., Xing, Y., Wang, Y., Phillips, N., Poffenberger, G., Johannesson, B., et al. (2018). β-cell replacement in mice using human type 1 diabetes nuclear transfer embryonic stem cells. Diabetes *67*, 26–35.

Tahtouh, T., Elkins, J.M., Soundararajan, M., Burgy, G., Durieu, E., Cochet, C., Schmid, R.S., Lo, D.C., Delhommel, F., et al. (2012). Selectivity, cocrystal structures, and neuroprotective properties of leucettines, a family of protein kinase inhibitors derived from the marine sponge alkaloid leucettamine B. J. Med. Chem. *55*, 9312–9330.

Talchai, C., Xuan, S., Lin, H.V., Sussel, L., and Accili, D. (2012). Pancreatic β cell dedifferentiation as a mechanism of diabetic β cell failure. Cell *150*, 1223–1234.

Tiwari, S., Roel, C., Wills, R., Casinelli, G., Tanwir, M., Takane, K.K., and Fiaschi-Taesch, N.M. (2015). Early and late G1/S cyclins and Cdks act complementarily to enhance authentic human β-cell proliferation and expansion. Diabetes *64*, 3485–3498.

Trachtman, H., Fervenza, F.C., Gipson, D.S., Heering, P., Jayne, D.R., Peters, H., Rota, S., Remuzzi, G., Rump, L.C., Sellin, L.K., et al. (2011). A phase 1, single-dose study of fresolimumab, an anti-TGF-β antibody, in treatment-resistant primary focal segmental glomerulosclerosis. Kidney Int. *79*, 1236–1243.

Wang, P., Alvarez-Perez, J.C., Felsenfeld, D.P., Liu, H., Sivendran, S., Bender, A., Kumar, A., Sanchez, R., Scott, D.K., Garcia-Ocaña, A., and Stewart, A.F.

(2015a). A high-throughput chemical screen reveals that harmine-mediated inhibition of DYRK1A increases human pancreatic beta cell replication. Nat. Med. *21*, 383–388.

Wang, P., Fiaschi-Taesch, N.M., Vasavada, R.C., Scott, D.K., García-Ocaña, A., and Stewart, A.F. (2015b). Diabetes mellitus–advances and challenges in human β-cell proliferation. Nat. Rev. Endocrinol. *11*, 201–212.

Wang, Y.J., Golson, M.L., Schug, J., Traum, D., Liu, C., Vivek, K., Dorrell, C., Naji, A., Powers, A.C., Chang, K.M., et al. (2016). Single-cell mass cytometry analysis of the human endocrine pancreas. Cell Metab. *24*, 616–626.

Wang, H., Bender, A., Wang, P., Karakose, E., Inabnet, W.B., Libutti, S.K., Arnold, A., Lambertini, L., Stang, M., Chen, H., et al. (2017). Insights into beta cell regeneration for diabetes via integration of molecular landscapes in human insulinomas. Nat. Commun. *8*, 767.

Xiao, X., Gaffar, I., Guo, P., Wiersch, J., Fischbach, S., Peirish, L., Song, Z., El-Gohary, Y., Prasadan, K., Shiota, C., and Gittes, G.K. (2014). M2 macrophages promote beta-cell proliferation by up-regulation of SMAD7. Proc. Natl. Acad. Sci. USA *111*, E1211–E1220.

Xiao, X., Fischbach, S., Song, Z., Gaffar, I., Zimmerman, R., Wiersch, J., Prasadan, K., Shiota, C., Guo, P., Ramachandran, S., et al. (2016). Transient suppression of TGFβ receptor signaling facilitates human islet transplantation. Endocrinology *157*, 1348–1356.

Yanagita, M. (2012). Inhibitors/antagonists of TGF-β system in kidney fibrosis. Nephrol. Dial. Transplant. *27*, 3686–3691.

Yang, X., Karuturi, R.K., Sun, F., Aau, M., Yu, K., Shao, R., Miller, L.D., Tan, P.B., and Yu, Q. (2009). CDKN1C (p57) is a direct target of EZH2 and suppressed by multiple epigenetic mechanisms in breast cancer cells. PLoS One *4*, e5011.

Zhou, J.X., Dhawan, S., Fu, H., Snyder, E., Bottino, R., Kundu, S., Kim, S.K., and Bhushan, A. (2013). Combined modulation of polycomb and trithorax genes rejuvenates β cell replication. J. Clin. Invest. *123*, 4849–4858.

Please cite this article in press as: Wang et al., Combined Inhibition of DYRK1A, SMAD, and Trithorax Pathways Synergizes to Induce Robust Replication in Adult Human Beta Cells, Cell Metabolism (2018), https://doi.org/10.1016/j.cmet.2018.12.005

STAR★METHODS

KEY RESOURCES TABLE

REAGENT or RESOURCE	SOURCE	IDENTIFIER
Antibodies		
Antibodies for Immunoblots		
Rabbit Monoclonal anti-SMAD 2/3 (D7G7)	Cell Signaling Technology	Cat#8685; RRID: AB_10889933
Rabbit Monoclonal anti-p-SMAD3 (p423+p425) (D27F4)	Abcam	Cat#Ab52903 Lot:GR128879-28; RRID: AB_882596
Rabbit Polyclonal anti-SMAD4 (B8)	Santa Cruz	Cat#Sc-7966 Lot: A2816; RRID: AB_627905
Rabbit Polyclonal anti-SMAD1/5/9	Abcam	Cat#ab66737 Lot:GR280688-13; RRID: AB_2192755
Rabbit Polyclonal anti-GAPDH (FL-335)	Santa Cruz	Cat#Sc-25778 Lot:13015; RRID: AB_10167668
Antibodies for Immunohistochemistry		
Rat Monoclonal anti-BrdU (ICR1)	Abcam	Cat#ab6326; RRID: AB_305426
Rabbit Monoclonal anti-Ki67 (Sp6)	Thermo Scientific	Cat#RM-9106 s1; RRID: AB_149792
Mouse Monoclonal anti-Ki67(MIB1),	DAKO	Cat# M7240 Lot: 20014345; RRID: AB_2142367
Rabbit Polyclonal anti-p-Histone-3	Millipore	Cat#06-570 Lot:GR273043-1; RRID: AB_310177
Polyclonal Guinea Pig Anti-Insulin	DAKO	Cat#A0564; RRID: AB_100113624
Mouse Monoclonal anti-p-γH2AX (3F2)	Thermo Scientific	Cat#MA1-2022: RRID: AB_559491
Mouse Monoclonal anti-NKX6.1	University of Iowa	Cat#F55A10-c; No RRID
Rabbit Polyclonal anti-PDX1	Millipore	Cat#07-696; RRID: AB_417404
Rabbit Polyclonal anti-MAFA	Abcam	Cat#Ab26405; RRID: AB_776146
Rabbit Monoclonal anti-Glucagon	Abcam	Cat#ab108426; RRID: AB_10887227
Rabbit Polyclonal anti-Somatostatin	Santa Cruz	Cat#Sc-20999 Lot: F707; RRID: AB_2195927
Rabbit Polyclonal anti-Pancreatic Polypeptide	DAKO	Cat#A0619 Lot:0111D; discontinued, No RRID
Rabbit Monoclonal anti-CK19	Abcam	Cat#Ab52625; RRID: AB_2281020
Secondary Antibody		
Species-specific mouse Alexa Fluor 488	Life Technologies	Cat#A-11029: RRID: AB_138404
Rat Alexa Fluor 594	Life Technologies	Cat#A-11007; RRID: AB_141374
Rabbit Alexa Fluor 488	Life Technologies	Cat#A11037; No RRID
Guinea pig Alexa Fluor 488	Life Technologies	Cat#A-11073; RRID: AB_142081
Antibodies for CHIP		
Rabbit Monoclonal anti-anti-SMAD2/3	Cell Signaling	Cat#8685; RRID: AB_10889933
Goat Polycolonal anti-SMAD4	R&D Systems	Cat#AF2097; RRID: AB_355150
Rabbit Polyclonal anti-KDM6A	Abcam	Cat#ab84190; RRID: AB_18611527
Rabbit Polyclonal anti-MEN1	Bethyl Laboratories	Cat#A300-105A; RRID: AB_2143306
Bacterial and Virus Strains		
Block-it Adenoviral RNAi expression system	Life Technologies	K494100; No RRID
pAd/CMV/V5-DEST Gateway Vector Kit	Lifetechnologies	V49320; No RRID
pAd/BLOCK-iT-DEST RNAi Gateway Vector	Lifetechnologies	V49220: No RRID
SMAD6 plasmid DNA	Harvard Plasmid Library BANK (https://plasmid.med.harvard.edu/PLASMID)	HsCD00325924; No RRID
SMAD7 Plasmid DNA	Harvard Plasmid Library BANK (https://plasmid.med.harvard.edu/PLASMID)	HsCD00345789; No RRID
Chemicals, Peptides, and Recombinant Proteins		
INDY	Tocris Biosciences	Cat#4997 CAS 1169755-45-6
BrdU substrate	GE Healthcare	Cat#RPN20
Harmine	Sigma	Cat#286044 CAS 442-51-3
Harmine.hydrochloride	This paper	CAS 343-27-1

(*Continued on next page*)

Continued

REAGENT or RESOURCE	SOURCE	IDENTIFIER
Leucettine-41	Adipogen	Cat#AG-MR-C0023-M005 CAS 112978-84-3
LY364947	Selleckchem	Cat#S2805
Alk5 inhibitor II	Cayman Chemical	Cat#14794 CAS*446859-33-2*
GW788388	Selleckchem	Cat#S2750 CAS 452342-67-5
A83-01	Tocris	Cat#2939 CAS 909910-43-6
SB431542	Selleckchem	Cat#S1067 CAS 301836-41-9
K02288	Selleckchem	Cat#S7359 CAS 1431985-92-0
LDN193189	Selleckchem	Cat#CA2618 CAS 1062368-24-4
Experimental Models: Cell Lines		
Human: HUES 8 hESC line (NIH approval number NIHhESC-09-0021)	HSCI iPS Core	hES Cell Line: HUES-8
Oligonucleotides		
Primers for CHIP		
CDKN1A_1 Forward ATGATCTCAGCTCACTGCAA	This paper	N/A
CDKN1A_1 Reverse ACAGGGTCAGGAGTTTTGAG	This paper	N/A
CDKN1A_2 Forward GGCTGCCTCTGCTCAATAATG	This paper	N/A
CDKN1A_2 Reverse ACAGGGTCAGGAGTTTTGAG	This paper	N/A
CDKN1A_3 Forward CTCCCCAAAGTAAAC AGAC	This paper	N/A
CDKN1A_3 Reverse CCAGCCCTTTGGATGGTTTG	This paper	N/A
CDKN1A_4 Forward CTGCTGGAACTCGGCCAGGCTCAG	This paper	N/A
CDKN1A_4 Reverse TGAGCTGCGCCAGCTGAGGTGTGA	This paper	N/A
CDKN1A_5 Forward CTAAAACAA GGGTTTGCG	This paper	N/A
CDKN1A_5 Reverse CTAGATCCTAGTCCTGTCTTGAAC	This paper	N/A
CDKN1A_6 Forward ACTTGTCCCTAGGAAAATCC	Koinuma et al., 2009	N/A
CDKN1A_6 Reverse GAAAACGGAGAGTGAGTTTG		N/A
shRNA against SMAD2 target sequence GCTGTAATCTGAAGATCTTCA	This paper	N/A
shRNA against SMAD3 target sequence GCAACCTGAAGATCTTCAACA	This paper	N/A
shRNA against SMAD4 target sequence GGAATTGATCTCTCAGGATTA	This paper	N/A
shRNA against CDKN1A target sequence CGCTCTACATCTTCTGCCTTA	This paper	N/A
shRNA against CDKN1C target sequence ATTCTGCACGAGAAGGTACAC	This paper	N/A

CONTACT FOR REAGENT AND RESOURCE SHARING

Requests for reagents and resources should be directed to and will be fulfilled by the Lead Contact, Andrew F. Stewart (andrew.stewart@mssm.edu).

EXPERIMENTAL MODEL AND SUBJECT DETAILS

Human Pancreatic Islet Studies

HIPPA-Compliant de-identified islets from 98 normal and six Type 2 diabetic adult cadaveric pancreas donors were obtained from the NIH/NIDDK-supported Integrated Islet Distribution Program (IIDP) (https://iidp.coh.org), from Dr. Tatsuya Kin at the University of Alberta, or from Dr. Patrick MacDonald at the Alberta Diabetes Institute. In all cases, informed written consent was provided at the institutions where the organs were harvested. For the normal doors, the mean age was 43.1 y.o. (range 16-68), 67 were male and 31 female, and the mean BMI was 30.5 (range 18.4-47.8). Sixty-six were Caucasian, 22 Hispanic/Latino, 6 Black, 3 Asian and 1 Pacific

Islander. The mean cold ischemia time was 509 min (range 210-1340). Purity ranged from 55%–99%. Among the Type 2 diabetes donors, the mean age was 53.8 y.o. (range 46-62), four were male and two were female, the mean BMI was 36.2 (range 32.5-42.8), and three were Caucasian and three were Hispanic. The mean HbA1c (±SEM) was 8.8 (±3.9), and three had had T2D for 0-5 years while the other three had had T2D for 6-10 years. Five of the six were on diabetes medications (1 on insulin, 4 on metformin, and 1 on an unknown diabetes medication). The causes of death were stroke (4), head trauma (1) and anoxia (1). Mean cold ischemia time was 367 min (range 352-384 min). Islet purity ranged from 55%–85%. Depending on the experiments performed, islets were used either as intact islets, or were first dispersed with Accutase (Sigma, St. Louis, MO) onto coverslips as described in the Figure Legends.

Mouse Studies

All studies were approved in advance by, and performed in compliance with, the Icahn School of Medicine at Mount Sinai Institutional Animal Care and Use Committee.

Normal Mouse Pancreas Studies

Male C57BL/6N mice (12-week-old) received vehicle (saline), 10 mg/kg harmine HCl, 30 mg/kg GW788388 or the combination of harmine and GW788388 by intraperitoneal injection daily for 7 days. Mice were sacrificed on day 7, pancreata harvested, fixed in 10% neutral buffered formalin, paraffin embedded and sectioned. Sections were stained for Ki67 and insulin as previously reported (Wang et al., 2015a). A minimum of 2,000 beta cells per pancreas was counted.

Mouse Partial Pancreatectomy (PPX) Studies

These studies were performed exactly as described previously (Wang et al., 2015a), with one exception: pancreas remnants were harvested at one week, rather than two weeks, following PPX. Briefly, 12 week old C57BL/6N mice underwent a sham or real 60% PPX. Seven days later, they were euthanized and the pancreas remnant harvested, weighed, fixed, sectioned, immunolabeled for insulin, beta cell area counted, and beta cell mass determined, all as described (Wang et al., 2015a).

NOD-SCID Mouse Studies

Male NOD-SCID mice (12 week old) were transplanted with human cadaveric islets in the left renal subcapsular space as described previously (Wang et al., 2015a). On postoperative day 7, they were randomized to receive vehicle (saline), 10 mg/kg harmine HCl, 30 mg/kg GW788388 or the combination of harmine and GW788388 by intraperitoneal injection daily for seven days. The renal grafts then were harvested, fixed, sectioned, immunolabelled for insulin and Ki67, and counted as described above, and as reported (Wang et al., 2015a). Five human islet donors were used in each of five sets of four NOD-SCID mice. A minimum of 2000 human beta cells were counted per graft. Investigators were blinded as to group assignments in all studies.

METHOD DETAILS

Adenoviruses and Transduction

Adenoviruses were prepared as described previously (Cozar-Castellano et al., 2004; Fiaschi-Taesch et al., 2009, 2013a, 2013b; Wang et al., 2015a, 2017). Unless otherwise described, all transductions were performed using 150 moi for two hours, and studies performed 96 hours later. The sequence and validation of the Ad.DYRK1A and Ad.shDYRK1A have been reported previously (Dirice et al., 2016; Wang et al., 2015a). Adenoviruses encoding human SMAD6 or SMAD7 were prepared using cDNAs encoding SMAD6 and SMAD7 obtained from Harvard PlasmID Database (https://plasmid.med.harvard.edu/). Adenoviruses employed for silencing SMADs 2,3 and 4 employed the DNA sequences in the Key Resources Table.

Quantitative PCR

RNA was isolated and quantitative RT-PCR was performed as described previously (Wang et al., 2015a). Gene expression in dispersed islets was analyzed by real-time PCR performed on an ABI 7500 System. Primers were as reported previously (Wang et al., 2015a) an in the Key Resources Table.

RNA sequencing

RNA from whole human islets (Tables S1 and S2) was prepared immediately using the RNeasy Micro kit (QIAGEN). Beta cell RNA yields were 300-500 ng from each FACS run, and RNA integrity numbers were between 9.5 and 10.0. PolyA$^+$ mRNA from sorted beta cells was purified with oligo dT magnetic beads. The polyA$^+$ RNA from beta cells was then fragmented in the presence of divalent cations at 94°C. The fragmented RNA was converted into double stranded cDNA. After polishing the ends of the cDNA, the 3′ ends were adenylated. Finally, Illumina-supplied universal adapters were ligated to the cDNA fragments. The adaptor ligated DNA was size selected to get an average of 250 bp insert size using AmpPure beads, and amplified by 15 cycle PCR. The PCR DNA was then purified using AmpPure beads to get the final seq library ready for sequencing. The insert size and DNA concentration of the seq library was determined on Agilent Bioanalyzer and Qubit, respectively. A pool of 10 barcoded RNA seq libraries was layered on two of the eight lanes of the Illumina flow cell at appropriate concentration and bridge amplified to yield ~25- 35 million raw clusters. The DNA reads on the flow cell were then sequenced on HiSeq 2000 using a 100 bp paired end recipe. Results are expressed as millions of counts (reads) per million bases (CPM).

Immunocytochemistry

Immunocytochemistry was performed on 4% paraformaldehyde fixed (15 min), Accutase-dispersed human islets plated on coverslips as described (Gaarenstroom and Hill, 2014; Micallef et al., 2012; Pagliuca et al., 2014; Tahtouh et al., 2012; Wang et al., 2015a, 2015b). Primary antisera are shown in the Key Resources Table. TUNEL labeling was performed as described (Gaarenstroom and Hill, 2014; Micallef et al., 2012; Pagliuca et al., 2014; Tahtouh et al., 2012; Wang et al., 2015a, 2015b).

Immunoblotting

Immunoblots were performed on whole human islets as described in detail previously (Cozar-Castellano et al., 2004; Fiaschi-Taesch et al., 2009, 2013a, 2013b; Wang et al., 2015a).

Glucose-Stimulated Insulin Secretion

GSIS was performed as described previously (Cozar-Castellano et al., 2004; Fiaschi-Taesch et al., 2009, 2013a, 2013b; Wang et al., 2015a). Briefly, whole human islets were cultured in low glucose (2.8mM) or high glucose (16.8 mM) for 30 min, and media harvested and assayed for insulin (Mercodia). Results are expressed as fold change in media insulin concentration in high glucose as compared to the low glucose concentration.

Proliferation in HUES8-Derived Human Beta Cells

Stem cell-derived beta cell proliferation assays were performed using three separate batches of cryopreserved cells. Differentiation of Harvard University embryonic stem 8 (HUES8) cells into beta cells was carried out as previously described (Millman et al., 2016; Pagliuca et al., 2014). Briefly, cryobanked SC-islet cells were thawed and aggregated in Stage 6 (S6) media (DMEM/F12 plus 1% HSA) for 8 −11 days in suspension culture. Clusters were then dissociated using Accutase (Innovative Cell Technologies, catalog #: AT-104) for 10 min and plated onto Matrigel- (Corning, catalog #: 354277) coated 96 well plates at a density of 1×10^5 cells/well in S6 media with 10 uM Y-27632. Following 24 hr of culture, compound treatment was initiated and lasted for four days with replenishment every other day. Cells were fixed with 4% paraformaldehyde for 15 min then stained overnight for insulin (Dako, A0564) and Ki67 (Thermo Scientific, RM-9106 s1) followed by fluorescent secondary antibodies (Thermo), anti-rabbit Alexa 594 and anti-guinea pig Alexa 488 and Hoescht (Thermo, H3569) staining. Beta cell proliferation (%insulin$^+$/Ki67$^+$) was quantified using a Multiwavelength Cell Scoring algorithm on the ImageXpress Micro 4 High-Content Imaging System (Molecular Devices) (Shen et al., 2015).

Expansion and Differentiation of Mel1-Derived Beta Cells: Stem cell line and culture

The Mel1 hESC line (Micallef et al., 2012) used in this manuscript is an NIH approved line (registry # 0139). hESC are grown on plates coated with primary mouse embryonic fibroblasts or MEFs (GlobalStem, CF-1 MEF IRR) and using human ES medium containing DMEM (GIBCO, 10569), 10% FBS (GE Healthcare, SH30088.03HI), 1% GlutaMAX (GIBCO, 35050061) and 1% Pen-Strep (Thermo Fisher Scientific, 15070-063). Cells are dissociated every 4-5 days using TrypLE Express (Life Technology, 12605036) for passaging. After dissociation, cells were suspended in human ES medium containing 10 μM ROCK inhibitor Y27632 (Selleckchem, S1049).

Differentiation of Mel1 Cells into Pancreatic Islets

Cells are grown to 80%–90% confluence, dissociated and suspended in mTeSR medium (STEMCELL Technology, 05850) with 10 μM ROCK inhibitor Y27632 (Selleckchem, S1049) and plated in a 1:1 ratio into Matrigel-coated (Fisher Scientific, 354277) wells for differentiation as previously described (Sui et al., 2018). The initial stages of differentiation were conducted in planar culture (d0-d11). For definitive endoderm stage (d1-d3) cells were cultured using STEMdiffTM Definitive Endoderm Differentiation Kit (StemCell Technologies, 05110). For primitive gut stage (d4-d6), cells were cultured in RPMI containing GlutaMAX (Life Technology, 61870-127), 1% (v/v) Penicillin-Streptomycin (PS) (Thermo Fisher Scientific, 15070-063), 1% (v/v) B27 Serum-Free Supplement (50x) (Life Technology, 17504044) and 50 ng/mL FGF7 (R&D System, 251-KG). For posterior foregut stage (d7-d8), cells were cultured in DMEM containing GlutaMax, 1% (v/v) PS, 1% (v/v) B27, 0.25 μM KAAD-Cyclopamine (Stemgent, 04-0028), 2 μM Retinoic acid (Stemgent, 04-0021) and 0.25 μM LDN193189 (Stemgent, 04-0074). For pancreatic progenitor stage (d9-d11), cells were cultured in DMEM containing GlutaMax, 1% (v/v) PS, 1% (v/v) B27 and 50 ng/mL EGF (R&D System, 236-EG). Cells were then dissociated using TrypLE Express (Life Technology, 12605036) and seeded into low-attachment 96 well-plates (Corning, 7007) (1 well of 6 well-plate to 60 wells of 96-well-plate) for clustering step to form aggregates or clusters of endocrine cells in DMEM containing GlutaMax, 1% (v/v) PS, 1% (v/v) B27, 0.25 μM Cyclopamine, 1 μM thyroid hormone (T3) (Sigma, T6397), 10 μM Alk5i, 10 μM Zinc sulfate (Sigma-Aldrich, Z4750) and 10 μg/mL Heparin (Sigma-Aldrich, H3149) for 2 days (d12-d13). For pancreatic endocrine stage (d14-20) cells were cultured using DMEM containing GlutaMax, 1% (v/v) PS, 1% (v/v) B27, 100 nM LDN, 1 μM T3, 10 μM Alk5i, 10 μM Zinc sulfate, 10 μg/mL Heparin and 100 nM gamma-secretase inhibitor (DBZ) (EMD Millipore, 565789). For mature pancreatic endocrine stage (d21-d27) cells were cultured using DMEM containing GlutaMax, 1% (v/v) PS, 1% (v/v) B27, 1 μM T3, 10 μM Alk5i, 10 μM Zinc sulfate, 10 μg/mL Heparin, 1 mM N-acetyl cysteine (N-Cys) (Sigma-Aldrich, A9165-5G), 10 μM Trolox (EMD Millipore, 648471-500MG) and 2 μM R428 (Tyrosine kinase receptor AXL inhibitor) (ApexBio, A8329). From d1 to d11 media was changed every day and from d12 to d27 media was changed every other day. All differentiations were done for 27 to 30 days. At Day 21, beta cell clusters were dissociated with trypsin and seeded at the exact same cell number (300-500,000 cells per well) into chambers on poly-D-lysine/laminin-coated slides and treated with either DMSO or the harmine-TGFβ inhibitor combination.

Flow Cytometry to Quantify Human Beta Cells

Human islets (250-300 IEQ) or stem cell-derived beta cells (300-500,000) were dispersed using Accutase (MT25058CI, Fisher Scientific) (for human islets) or trypsin (for hESC-derived beta cells) and plated on laminin/poly-D-lysine coated chamber slides (BD354688, VWR Scientific). For human islets, beta cells were labeled with an adenovirus as described previously (Wang et al., 2017). Briefly, human islet cells were dispersed to single cells in eigth-well chambers and transduced for two hours in RPMI1640 medium without fetal bovine serum (FBS) with 150 moi of an adenovirus expressing the bright green fluorescent protein, ZsGreen (Clontech, Mountain View CA), under control of the rat insulin-1 promoter (RIP1) and a mini-CMV enhancer (Wang et al., 2017). The RIP1-miniCMV promoter included 177 bases of the hCMV IE-1 promoter ClaI-SpeI fragment ligated to 438 bases of the RIP1 promoter. The beta cell fraction was confirmed to be > 92% pure by immunolabeling of sorted cells with insulin, by qRT-PCR and by RNaseq (Figure S7) (Wang et al., 2017). Following transduction with the Ad.RIP-ZsGreen adenovirus for two hours, 300 μL of RPMI1640 medium containing 10% FBS was added to terminate adenovirus infection, and cells were allowed to express ZsGreen for 24 hours. At this point, fresh medium containing DMSO or harmine 10μM, Ly364947 3μM or the harmine-LY combination was added for another four days. Human Mel1-ES cell-derived beta cells were labeled with endogenous GFP (Sui et al., 2018).

For flow cytometric human beta cell quantification, following four days (for human islet cells) or seven days (for hESC-derived beta cells) of drug treatment (DMSO or harmine + LY364947), cells were harvested by gentle Accutase (for human beta cells) or trypsin (for hESC-dervied beta cells) dissociation and 50,000 fluorescent beads (ACURFP-50-10, Spherotech) were added, serving as an internal recovery standard and FACS counting reference. DAPI (D3571, Life Technologies) was used as a dead/live cell marker. Dispersed cells were loaded onto an Aria II cell sorter, and live $ZsGreen^+$ (from human islets) or GFP^+ (from hESC) cells were counted until 10,000 beads had been counted from each the vehicle- and the harmine-LY364947-treated wells. Results are expressed as absolute numbers of $ZsGreen^+$ or GFP^+ beta cells, corrected to the 50,000 original internal bead standard. The beta cell fraction was confirmed to be > 92% pure by immunolabeling of sorted cells with insulin, by qRT-PCR and by RNaseq (Wang et al., 2017).

Chromatin Immunoprecipitation (ChIP) Assays

ChIP was performed using the EZ-ChIP Kit (#Magna0001, Millipore) according to manufacturer's protocol as described previously (Wang et al., 2017). Whole human cadaveric islets were dispersed as described previously. A minimum of three separate islet preparations were used for each figure shown. $2x10^6$ cells were collected per experiment for each SMAD2/3, SMAD4, KDM6A and MEN1 immunoprecipitation. Immunoprecipitated DNA was quantified using ABI 7500 real-time quantitative PCR detection system (Life Technologies). Data are presented as binding signals calculated by normalizing the ChIP signals relative to input controls and subsequently subtracting the IgG value from the respective antibody. The resulting values below zero indicated no binding and depicted as 'zero' in ChIP plots. Error bars indicate mean ± SEM. The primer sets for *CDKN1A* and *CDKN1C* were described previously (Koinuma et al., 2009; Wang et al., 2017; Yang et al., 2009). The antibodies and the primer sequences used are described in the Key Resources Table.

QUANTIFICATION AND STATISTICAL ANALYSIS

Statistics

Statistics were performed using Student's two-tailed paired t test (for paired samples) or by One-Way Analysis of Variance for repeated-measures for multiple comparisons, as described in the Figure Legends. P values less than 0.05 were considered to be significant.

DATA AND SOFTWARE AVAILIBILITY

RNaseq data re available in Tables S1 and S2.